

Knowledge-Based Prediction of Network Controllability Robustness

Yang Lou, Yaodong He, Lin Wang, *Member, IEEE*, Kim Fung Tsang, *Senior Member, IEEE*, and Guanrong Chen, *Life Fellow, IEEE*

Abstract—Network controllability robustness reflects how well a networked system can maintain its controllability against destructive attacks. Its measure is quantified by a sequence of values that record the remaining controllability of the network after a sequence of node-removal or edge-removal attacks. Traditionally, the controllability robustness is studied only for directed networks and is determined by attack simulations, which is computationally time consuming or even infeasible. In the present paper, an improved method for predicting the controllability robustness of undirected networks is developed based on machine learning using a group of convolutional neural networks (CNNs). In this scheme, a number of training data generated by simulations are used to train the group of CNNs for classification and prediction, respectively. Extensive experimental studies are carried out, which demonstrate that 1) the proposed method predicts more precisely than the classical single-CNN predictor; 2) the proposed CNN-based predictor provides a better predictive measure than the traditional spectral measures and network heterogeneity.

Index Terms—Knowledge-based prediction, complex network, convolutional neural network, controllability, robustness.

1 INTRODUCTION

COMPLEX networks as an interdisciplinary research field has gained growing popularity since the late 1990s, encompassing network science, systems engineering, applied mathematics, statistical physics, and biological as well as social sciences [1]–[4]. Scientific studies are trying to understand the essence and characteristics of complex networks while engineering studies are trying to control them for beneficial applications. In the pursuit of networked systems control, whether or not they can be controlled is a fundamental issue, which leads to the basic concept of network controllability [5]–[15].

The concept of *controllability* refers to the ability of a system or a network of systems in changing from any initial state to any desired state under a feasible control input in finite time [15]. In retrospect, it was shown [5] that identifying the minimum number of external control inputs (recalled driver nodes), needed to achieve the *structural controllability* of a *directed* network, which requires searching for a maximum matching of the network. Thereafter, in [6], an efficient measure is introduced for assessing the *state controllability*, based on the rank of the network controllability matrix, for both *directed* and *undirected* networks.

It took quite a long time for people to understand the intrinsic relation between topology and controllability of a

general, mostly directed network. It was found that clustering and modularity have no prominent impact on the network controllability, but degree correlation has a certain effect [7]. It was revealed [8] that random networks of any topology are controllable by an extremely small number of driver nodes if both of its minimum in- and out-degrees are bigger than two. A control centrality was introduced in [16] to measure the importance of nodes regarding their roles against random attacks. The network controllability of some canonical graph models is studied and compared in [17]. For growing networks, the evolution of network controllability is investigated in [18]. Moreover, the controllability of multi-input/multi-output networked systems is studied in [10], [19], with necessary and sufficient conditions derived. Recently, it was realized that some special motifs such as loops and chains are beneficial for enhancing the robustness of network controllability against attacks [20]–[22]. A comprehensive survey of the subject is presented in [15].

Regarding the robustness of network controllability against attacks, which includes random failures and malicious destructions, a large number of studies have been reported [16], [23]–[27]. For node-removal or edge-removal attacks, the main issue is to develop a measure that reflects how well the networks can maintain their controllability after the attacks took place. One measure for the network controllability is quantified by the number of external control inputs needed to recover or retain the network controllability after the occurrence of an attack, while its robustness is quantified by a sequence of values that record the remaining levels of the network controllability after a sequence of attacks [21]. To optimize the network robustness, one usually aims to enhance and maintain a highest possible *connectedness* of the network against attacks [25]. Given a degree-preserving requirement or constraint (i.e., the degree of each node remains unchanged through the process

• Y. Lou, Y. He, K.F. Tsang and G. Chen are with the Department of Electrical Engineering, City University of Hong Kong, Hong Kong, China.

E-mails: felix.lou@my.cityu.edu.hk; yaodonghe2-c@my.cityu.edu.hk; ee330015@cityu.edu.hk; eegchen@cityu.edu.hk.

• L. Wang is with the Department of Automation, Shanghai Jiao Tong University, Shanghai 200240, China, and also with the Key Laboratory of System Control and Information Processing, Ministry of Education, Shanghai 200240, China.

E-mail: wanglin@sjtu.edu.cn.

Corresponding author: Guanrong Chen.

of optimization), an edge-rewiring method is proposed in [28], which increases the number of edges between high-degree nodes, so as to generate a new network with a largest k -shell component. In [29], the structure of a network is modified by degree-preserving edge-rewiring, where a spectral measure is used for optimization. By optimizing a specified spectral measure of the network through random edge-rewiring, the robustness of the resultant network is enhanced consequently. However, it was noted that the correlation between spectral measures and the robustness is indeed unclear [30]. Nevertheless, given a reliable predictive measure or indicator of the network robustness, optimization algorithms can be applied [31]–[34]. In the case that there are more than one predictive measure, multi-objective optimization schemes can be adopted [35]. In [36], it is shown that network robustness against edge- and node-removals can be enhanced simultaneously. A common observation is that heterogeneous networks with onion-like structures are robust against attacks [25], [37]–[39]. The evolution of alternative attack and defense is studied in [40], where attack refers to edge-removal and defense means edge-replenishment. The connectedness of the largest-sized cluster is a commonly-used measure for such robustness [25]. It is noted that, although the robustness of network connectedness has a certain positive correlation with the robustness of the network controllability, they have very different characteristics and measures.

Although the correlation between network topology and network controllability has been investigated, no specific theoretical indicator or performance index was found that can precisely quantify the general network controllability robustness. Under different types of attacks, the robustness of network controllability behaves differently. The nature of the attack methods leads to different measures of the *importance* of a node (or an edge) in a network. In the literature, degree and betweenness are two commonly-used measures for the importance of nodes and edges, respectively [41].

It was observed that a power-law degree distribution does not necessarily imply a fragile controllability robustness against targeted node-removals; what really contributes to enhance the network controllability robustness is the multiple-chain structure [42] and multi-loop structure [20], [21]. Later, it was observed [22] that it is particularly beneficial to the network controllability robustness if the multiple-loops are across the entire networks rather than only within local communities. Lately it was empirically observed [43] that to achieve optimal controllability robustness against random node attacks, both in- and out-degrees of a directed network should be extremely homogeneous.

On the other hand, in the field of machine learning, deep neural networks have shown powerful capability in performing classification and regression tasks in image processing. Convolutional neural network (CNN) is one kind of effective deep neural network [44]. CNN is able to automatically analyze inner features of a dataset without human interference. But, if the user has some prior knowledge and it can be ensured that such prior knowledge would not mislead machine learning, then CNN will become even much powerful for data analysis and processing. Successful real-world applications of CNNs include text recognition and classification [45]–[47], face recognition and detection

[48], collective classification [49], air quality forecasting [50], etc.

Traditionally, for large-scale complex networks, their controllability robustness is evaluated and predicted by attack simulations, which however are extremely computationally time consuming. To improve the efficiency of prediction for the network controllability robustness, this paper takes a machine learning-based approach to designing a knowledge-based predictor for the controllability robustness (iPCR), which is an improved version of the single CNN-based predictor of the controllability robustness (PCR) developed in [51], taking advantage of available prior knowledge.

One unique feature of this iPCR is that it can be applied to both directed and undirected networks, since there is no essential difference for the CNN to process an image converted from a directed or an undirected network, where the symmetry in the network-converted image does not affect the learning of the CNN. As such, the proposed iPCR has a much wider application range than other traditional methods.

Another improved mechanism in iPCR is that the network-converted images are updated independently of the generation process. This is illustrated by Fig. 1, where in the upper row there are intrinsic features of the images pertaining to the generation of the network. These biased features are filtered out by shuffling the rows and columns of the image, as shown in the lower row of the figure. For example, in a Barabási-Albert (BA) scale-free network, the preferential attachment mechanism gives the ‘old’ nodes higher degrees, which are usually allocated near each other therefore have small numbers in the adjacency matrix. As a result, there are always some sparks in the BA-converted image, as shown in Fig. 1 (a). The generation-based features necessarily mitigate the task of a CNN in classification and regression. Therefore, in the iPCR, these special features are filtered out by shuffling the rows and columns of the images, as shown in the lower row of Fig. 1.

To briefly summarize, the proposed design of the iPCR is based on the following observations: 1) there is no clear correlation between the topological features and the controllability robustness of a general network, directed or undirected, 2) the adjacency matrix of a network can be equivalently represented as a gray-scale image, 3) the CNN technique has proved successful in image processing without human intervention, and 4) prior knowledge at hand could be sufficiently utilized as preprocessing and filtering tools. In the iPCR, a number of training data generated by simulations are used to train the group of CNNs for classification and prediction, respectively.

Extensive experimental studies are carried out, which demonstrate that 1) the proposed method predicts more precisely than the single-CNN predictor; 2) the CNN-based prediction method provides a better predictive measure than the traditional spectral measures and network heterogeneity.

The rest of the paper is organized as follows. Section 2 reviews the network controllability and its robustness against various destructive attacks. Section 3 introduces the proposed iPCR. In Section 4, experimental study is performed with analysis. Finally, Section 5 concludes the

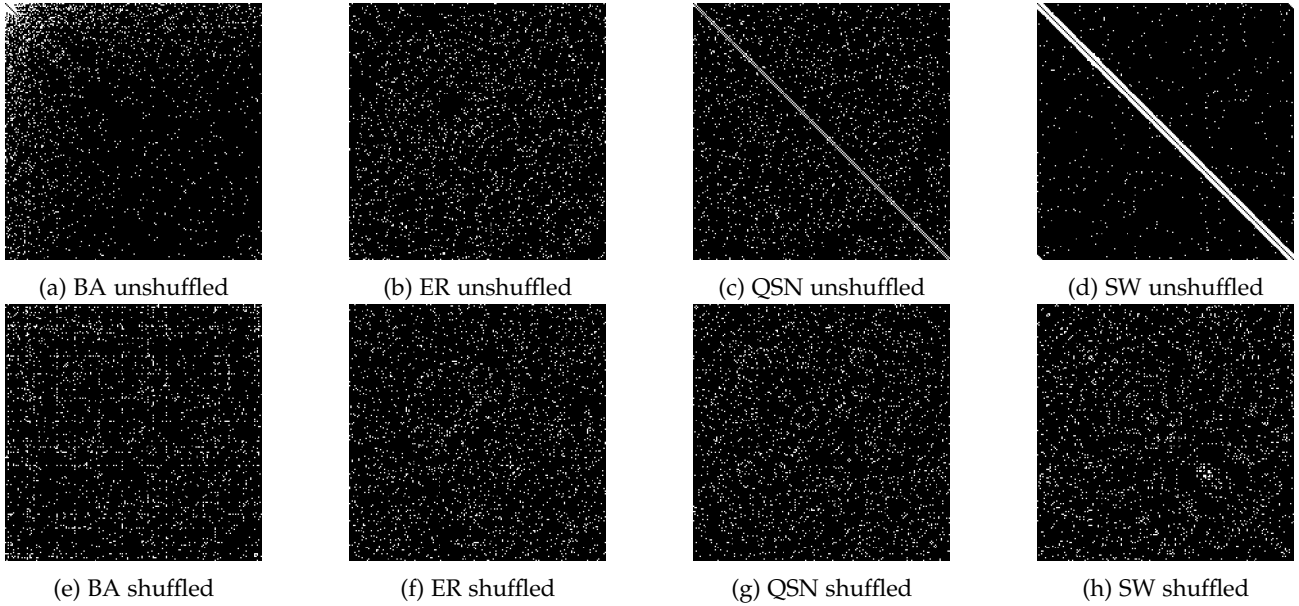


Fig. 1: An example of converting an adjacency matrix to an image, for both weighted and unweighted image cases. The network size $N = 200$ with average degree $\langle k \rangle = 5.12$. In each image, a black pixel represents a 0 element in the adjacency matrix; a white pixel represents a 1 element in the unweighted network.

investigation.

2 NETWORK CONTROLLABILITY AND ITS ROBUSTNESS

Consider a linear time-invariant networked system described by $\dot{\mathbf{x}} = A\mathbf{x} + B\mathbf{u}$, where A and B are constant matrices of compatible dimensions, \mathbf{x} is the state vector, and \mathbf{u} is the control input. The system is *state controllable* if and only if the controllability matrix $[B \ AB \ A^2B \ \dots \ A^{N-1}B]$ has a full row-rank, where N is the dimension of A , also the size of the networked system. If a system is state controllable, then its state vector \mathbf{x} can be driven from any initial state to any desired state in the state space by a suitable control input \mathbf{u} within finite time. The concept of structural controllability is a slight generalization dealing with two parameterized matrices A and B , in which the parameters characterize the structure of the underlying networked system: if there are specific parameter values that can ensure the parametric system be state controllable, then the system is *structurally controllable*.

The controllability of a network, or networked system, is measured by the density of the controlled nodes, n_D , defined by

$$n_D \equiv \frac{N_D}{N}, \quad (1)$$

where N_D is the number of external control inputs (driver nodes) needed to retain the network controllability, and N is the network size. This measure n_D allows networks with different sizes can be compared. The network size does not change at a step with an edge-removal attack but would be reduced by a node-removal attack. In comparison, the smaller the n_D value is, the better the network controllability will be.

For a directed network, the number N_D can be calculated according to the *minimum inputs theorem* derived

based on maximum matching [5]. A maximum matching is a matching that contains the largest possible number of edges, which cannot be further extended in the network. A node is matched if it is the end of an edge in the matching; otherwise, it is unmatched. When a maximum matching is found, the number N_D of driver nodes is determined by the number of unmatched nodes, i.e. $N_D = \max\{1, N - |E^*|\}$, where $|E^*|$ is the number of edges in the maximum matching E^* .

As for an undirected network, its controllability can be calculated according to the *exact controllability theorem* derived based on the controllability matrix [6]. Given an undirected sparse network, its number N_D of driver nodes is calculated by

$$N_D = \max\{1, N - \text{rank}(A)\}. \quad (2)$$

Here, a network is considered to be sparse if the number of edges M , i.e., the number of nonzero elements in the adjacency matrix, is much smaller than the possible maximum number of edges, $M_{\max} = N \cdot (N - 1)$. Practically, if $M/M_{\max} \leq 0.05$, then it can be considered as a sparse network.

The measure of controllability robustness is calculated by

$$n_D(i) \equiv \frac{N_D(i)}{N - i}, \quad i = 1, 2, \dots, N - 1, \quad (3)$$

where $N_D(i)$ is the number of driver nodes needed to retain the network controllability after a total of i nodes have been removed, and N is the original network size. When these values are plotted, a curve is obtained, called the *controllability curve*.

To compare the controllability robustness of two networks against the same attack sequence, their controllability curves are plotted against each other for better visualization. Numerically, a controllability curve c is given by an $(N - 1)$

vector $n_D^c = [n_D^c(1), n_D^c(2), \dots, n_D^c(N-1)]$. Thus, given two network controllability curves, c_1 and c_2 , the difference (error) of the two curves, when the same number of i nodes are removed, is calculated by

$$\sigma(i) = |n_D^{c_1}(i) - n_D^{c_2}(i)|. \quad (4)$$

The average error $\bar{\sigma}$ is then calculated by

$$\bar{\sigma} = \frac{1}{N-1} \sum_{i=1}^{N-1} \sigma(i). \quad (5)$$

The vector $\sigma(i)$ is used to measure the error between the predicted controllability curve against the true curve; while the scalar $\bar{\sigma}$ measures the overall error of prediction.

The overall robustness of network controllability R_c is defined as [27], [52]

$$R_c = \frac{1}{N-1} \sum_{i=1}^{N-1} n_D(i), \quad (6)$$

where, as an extension of the robustness measure defined in [25], $n_D(i)$ represents the controllability of the network when a total of i nodes have been removed from the network. Given two complex networks under the same attack, the one with a lower R_c value is considered having better controllability robustness.

In the following, for convenience in description, sometimes the integer index sequence $i = 1, 2, \dots, N-1$ will be replaced by the fractional index sequence $p = \frac{1}{N}, \frac{2}{N}, \dots, \frac{N-1}{N}$, thereby equivalently replacing $n_D(i)$ ($i = 1, 2, \dots, N-1$) with $n_D(p)$ ($p = \frac{1}{N}, \frac{2}{N}, \dots, \frac{N-1}{N}$).

3 PREDICTOR FOR NETWORK CONTROLLABILITY ROBUSTNESS

3.1 Framework of Predictor

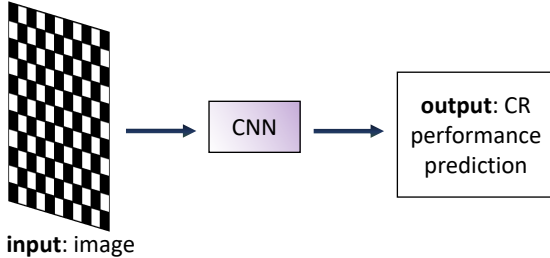


Fig. 2: The framework of PCR [51], where a single CNN is used for controllability robustness (CR) prediction. The input is an image converted from the adjacency matrix; the output is the corresponding CR curve.

The framework of PCR is shown in Fig. 2, where a single CNN is trained for prediction, referred to as a *predictor*. This framework straightforwardly performs fairly good predictions, with an overall error less than the standard deviation of the testing samples [51]. However, there are two main issues about this framework. First, many of the PCR predicted controllability curves are vibrating (especially in the initial stage of the attacks), while the real controllability curves are generally smooth. Second, PCR ignores all available prior

knowledge, and trains the single CNN using the raw data without any preprocessing.

To address the first issue, in the new framework a data processor called *filter* is installed after the prediction and before the output. Using available prior knowledge about the dynamics, upper and lower boundaries of the controllability curve can be pre-set. Specifically, during a node-removal attack process, where i ($i = 1, 2, \dots, N-1$) nodes are removed, the upper and lower bounds of the controllability curve at position i are pre-set as follows:

$$ub(i) = \frac{\min(N_D^0 + i, N-i)}{N-i}, \quad (7)$$

and

$$lb(i) = \frac{1}{N-i}, \quad (8)$$

where $ub(i)$ and $lb(i)$ represent the upper and lower bounds of $n_D(i)$, respectively; N_D^0 means the minimum required number of driver nodes for the original network before being attacked, which can be calculated by Eq. (2).

The following boundary processor is designed:

$$n'_D(i) = \begin{cases} ub(i), & \text{if } n_D(i) > ub(i), \\ lb(i), & \text{if } n_D(i) < lb(i). \end{cases} \quad (9)$$

Based on this, a median filter with a mask length L is implemented.

To address the second issue, although human-intervention-free is one of the most attractive properties of deep learning, some available knowledge and common sense may be used if such human knowledge would not mislead the machine learning process. Such prior knowledge of the network data will be preprocessed before prediction. For instance, if the network topology is known beforehand, then the prediction work can be passed to a CNN that is specialized for such a topology, which can have better prediction performance.

The framework of iPCR consists of a group of CNNs, including a *classifier* (used for data classification) and several predictors, as shown in Fig. 3. Compared to PCR, iPCR first checks the classifiability of the input data. The classifier CNN_c is trained by applying the prior knowledge of the user. If an input is classifiable and belongs to a specific data cluster, then it will be passed to the specific CNN_i ($i = 1, 2, \dots, nc$, where nc is the number of clusters) for prediction; otherwise, the input is passed to a general CNN_{all}, which is trained in exactly the same way as the CNN in PCR. Each CNN_i ($i = 1, 2, \dots, nc$) is then trained by the specific cluster of data, such that it is specialized in predicting a cluster, although probably not suitable for another.

In the experimental study, two types of prior knowledge are tested, namely the network topology (presented in Sec. 4) and the node degree (presented in Supplementary Information (SI) due to space limitation in the paper). Experimental results show that the former provides helpful prior knowledge, while the later is misleading and consequently the prediction results are degenerated.

Finally, before outputting the predicted results, iPCR operates a filter that includes a boundary processor (as shown in Eq. (9)) and a median filter.

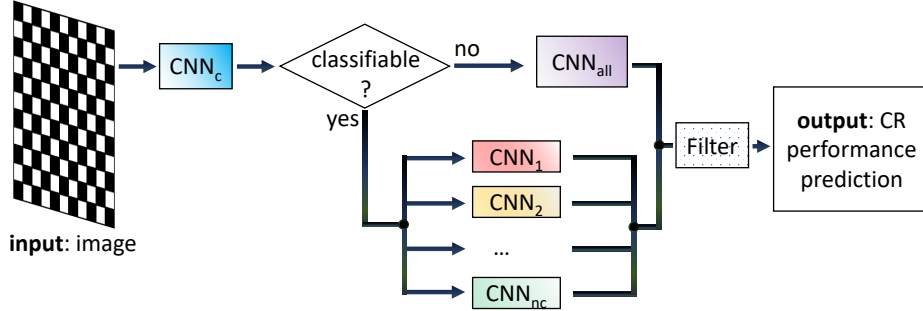


Fig. 3: The framework of iPCR, where a CNN_c is used for data classification. If the input data can be clearly classified as one specific group, then iPCR uses a specifically trained CNN_i , $i = 1, 2, \dots, nc$, where nc is the number of clusters; otherwise, if the input data is non-classifiable based on the current knowledge, then iPCR degenerates to PCR using a single CNN_{all} .

3.2 Convolutional Neural Network

The CNN framework, which includes a classifier, several predictors and a filter, is now introduced along with its configuration and parameter settings.

TABLE 1: Parameter settings of the seven groups of convolutional layers.

Group	Layer	Kernel size	Stride	Output channel
Group 1	Conv7-64	7x7	1	64
	Max2	2x2	2	64
Group 2	Conv5-64	5x5	1	64
	Max2	2x2	2	64
Group 3	Conv3-128	3x3	1	128
	Max2	2x2	2	128
Group 4	Conv3-128	3x3	1	128
	Max2	2x2	2	128
Group 5	Conv3-256	3x3	1	256
	Max2	2x2	2	256
Group 6	Conv3-256	3x3	1	256
	Max2	2x2	2	256
Group 7	Conv3-512	3x3	1	512
	Max2	2x2	2	512

Figure 4 shows the detailed CNN structure. The detailed parameter settings of the 7 groups of convolutional layers are given in Table 1. Here, the CNN architecture follows the Visual Geometry Group (VGG)¹) architecture [53]. The number of feature map (FM) groups is set to 7, since the input size is 1000×1000 in the following experiments. Note that this number should be set to be greater for a larger input dataset. Each FM consists of a convolution layer, a ReLU, and a max pooling layer. A ReLU provides a commonly-used activation function $f(x) = \max(0, x)$ [54]. The output of each hidden layer, i.e., a multiplication of weights, is summed up and then rectified by the ReLU for the next layer. The max pooling layer reduces the dimension of the dataset for the input to the next layer.

For prediction, following the FM groups, the fully-connected layer outputs an $(N - 1)$ vector that represents the predicted controllability curve; while for classification, an extra softmax layer [55] is attached at the end such that the output is a vector of nc real numbers. Moreover, pl_i ($\sum_{i=1}^{nc} pl_i = 1$) represents the probability that the input image belongs to cluster i , $i = 1, 2, \dots, nc$. A threshold

$\eta = 0.8$ is set such that, only if there exists a $pl_i \geq \eta$ ($i = 1, 2, \dots, nc$), it returns a result indicating that the input image is classifiable (belonging to cluster i); otherwise, the input is recognized as non-classifiable.

Note that for different purposes, the internal weights of the CNN will be set differently. Here, for illustration, the structures of predictors and classifiers are plotted together. But a predictor and a classifier do not share any internal weight, and each CNN works (including training and testing) independently in the proposed iPCR.

The loss function used in the classifier is the cross entropy. Given the predicted and the true probability distribution of an instance, denoted by pl and tl respectively, the cross entropy of this instance is calculated as follows:

$$H = - \sum_{i=1}^{nc} tl(i) \cdot \log[pl(i)]. \quad (10)$$

The loss function used in the predictor is equal to the mean-squared error between the predicted controllability curve pv and the true curve tc , which is calculated as follows:

$$\mathcal{L} = \frac{1}{N-1} \sum_{i=1}^{N-1} \|pv(i) - tv(i)\|, \quad (11)$$

where $\|\cdot\|$ is the Euclidean norm.

The training process for the classifier and predictor aims to minimize the cross entropy in Eq. (10) and the mean-squared error in Eq. (11), respectively.

4 EXPERIMENTAL STUDIES

4.1 Experimental Settings

Four typical undirected synthetic networks are adopted for simulation, namely the Barabási–Albert (BA) scale-free network [56], Erdős–Rényi (ER) random-graph network [57], q -snapback network (QSN) [20], [22], and Newman–Watts (NW) small-world network [58].

In the following subsections, the generation methods and parameter settings of the above four networks are introduced, respectively.

Note that, given the network size N and average degree $\langle k \rangle$, there are $M = \lfloor N \cdot \langle k \rangle \rfloor$ edges in total. Standard notation $\lfloor \cdot \rfloor$ and $\lceil \cdot \rceil$ represent the floor and ceiling functions, respectively.

1. <http://www.robots.ox.ac.uk/~vgg/>

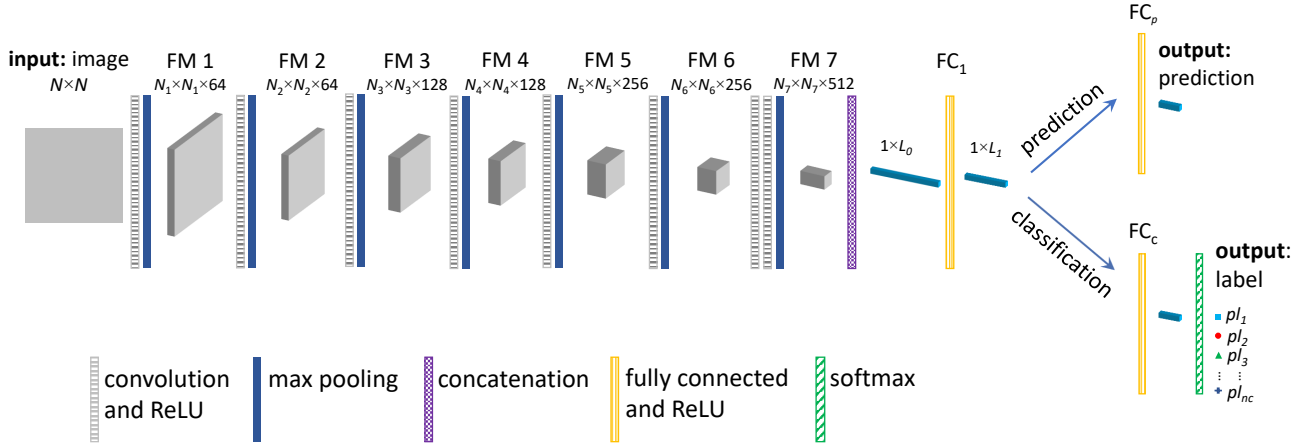


Fig. 4: [Color online] The architecture of the CNN used for networks classification and controllability robustness prediction, where FM is an abbreviation for *feature map*, and FC for *fully connected*. The data sizes $N_i = \lceil N/(i+1) \rceil$, $i = 1, 2, \dots, 7$. The concatenation layer rearranges the matrix into a vector, from FM 7 to FC 1, i.e., $L_0 = N_7 \times N_7 \times 512$. $L_2 \in (L_0, N-1)$ is a hyperparameter. Set $L_2 = 4096$ in this paper. For prediction, another fully-connected layer FC_p is used as the output layer, yielding an $(N-1)$ vector in the output. For classification, a fully-connected layer FC_c followed by a softmax layer is used. The output is the labeled according to the input data.

4.1.1 Barabási–Albert (BA) Scale-Free Network

A BA network is generated as follows:

- Start with n_0 fully-connected nodes (i.e., an n_0 -clique).
- For nodes i ($i = n_0 + 1, \dots, N$), each of them connects to each of nodes j ($j = 1, \dots, i-1$) with a probability of $p_{BA} = \frac{k_j}{\sum_l k_l}$, where k_j denotes the degree of node j . At each step, there are e_{BA} edges being added preferentially.

Set $n_0 = \lceil \langle k \rangle \rceil + 1$ and $e_{BA} = \frac{M - \binom{n_0}{2}}{N - n_0}$. To exactly control the number of the generated edges to be M , proportionally adding or removing edges can be performed.

4.1.2 Erdős–Rényi (ER) Random-Graph Network

An ER network is generated as follows:

- Start with N isolated nodes.
- Pick up all possible pairs of nodes from the N given nodes, denoted as i and j ($i \neq j, i, j = 1, 2, \dots, N$), once and once only. Connect each pair of nodes with a probability $p_{ER} \in [0, 1]$.

Let $p_{ER} = \frac{\langle k \rangle}{N-1}$. To exactly control the number of the generated edges to be M , uniformly-randomly adding or removing edges can be performed.

4.1.3 q -Snapback Network

The q -snapback network (QSN) was originally constructed as a directed network [20] but is converted to be an undirected one here, with only one layer r_{QSN} for simplicity. It is generated as follows:

- Start with a chain of N nodes, where each node i ($i = 2, \dots, N-1$) has two edges connecting to its neighboring nodes $i-1$ and $i+1$.
- For each node $i = r_{QSN} + 1, r_{QSN} + 2, \dots, N$, it connects backward to the previously-appeared nodes

$i - l \times r_{QSN}$ ($l = 1, 2, \dots, \lfloor i/r_{QSN} \rfloor$), with the same probability $q \in [0, 1]$.

The probability parameter q can be calculated from the given N , M , and r_{QSN} . For $r_{QSN} = 1$, $q = \frac{(M-N) \cdot r_{QSN}}{\sum_{j=2+r_{QSN}}^{N-2} j} = \frac{M-N}{\sum_{j=3}^{N-2} j}$. To exactly control the number of the generated edges to be M , uniformly-randomly adding or removing edges can be performed.

4.1.4 Newman–Watts (NW) Small-World Networks

An NW network is generated as follows:

- Start with an N -node loop having K connected nearest-neighbors on each side.
- Some edges are added without removing any existing edges, until totally M edges have been added.

Set $K = 2$ in the following; that is, a node i is connected to its two nearest neighbors on each side, i.e., with nodes $i-1, i+1, i-2$ and $i+2$.

Since the above generation methods will generate networks with some strong visible features (as illustrated by Fig. 1), the rows and columns of the resulting adjacency matrices are shuffled, so as to filter out these features. It should be noted, however, that after shuffling the neighboring relationship will be changed. For example, in QSN, the starting chain remains, which connects all the N nodes, but now it is not necessary that node i (the i th row and column in the adjacency matrix) remains to connect nodes $i-1$ and $i+1$ like before.

Next, in Sec. 4.2, the performances of PCR and iPCR are compared on predicting the controllability robustness of unweighted networks against random node-removal attacks. Then, in Sec. 4.3, PCR and iPCR are compared on predicting the controllability robustness of weighted networks against targeted node-removal attacks. In these two experimental studies, PCR and iPCR aim to predict the

precise controllability curves. Finally, in Sec. 4.4, PCR and iPCR are compared on predicting the ordinal ranks of the network controllability robustness, and compared to 6 spectral measures and the heterogeneity.

In all the following comparisons, a filter consisting of a boundary processor and a median filter (with $L = 9$) are installed in both PCR and iPCR.

4.2 Unweighted Networks under Random Attacks

The controllability robustness prediction on unweighted networks with size $N = 1000$ and average degree $\langle k \rangle = 3, 4, 5$, under random node-removal attacks, is studied.

There are 12 network configurations in total. For each configuration, 500 training samples are used. Each sample includes an adjacency matrix (as the input) and its controllability robustness curve obtained from simulation (as the output). CNN_{all} of iPCR is trained by $12 \times 500 = 6000$ training samples; while each of CNN_{1,2,3,4} is trained by $3 \times 500 = 1500$ samples. Each CNN_k ($k = 1, 2, 3, 4$) is specifically trained for one of the four network types, namely BA, ER, QSN, and NW; while CNN_{all} is trained by the ensemble of all the networks. PCR is trained in the same way as CNN_{all} of iPCR. Given a random attack, in simulation the result is averaged from 10 independent runs, so as to balance mitigating and randomness influences, which also reduces the burden of computation.

Another set of 100 testing samples for each network configuration are generated independently. The classification results of CNN_c are shown in Table 2. As illustrated by Fig. 1, shuffling filters out the method-generated features in the resultant images, which however makes the classification task becoming tougher. It can be seen from the figure that CNN_c correctly classifies the four types of networks at a successful rate higher than 0.8333, resulting images indistinguishable by eyes. Since the threshold is set to $\eta = 0.8$ in the softmax layer of the classifier, an input is non-classifiable if it generates a result with the probability of success greater than 0.8, and in this case the input is considered being correctly predicted by the CNN_{all}. As can be seen from Table 2, the rate of non-classifiable (NC) data is low, indicating the effectiveness of the classifier which uses prior knowledge.

Note that if an input is incorrectly classified, it will be passed to a wrong predictor that is specialized for a different network type. This will totally mislead the prediction, and therefore is harmful particularly if the error rate is high. In iPCR, according to Table 2, BA and QSN may be misclassified as ER at rates 0.0922 and 0.0165, respectively; NW may be mis-classified QSN at a rate 0.0042; ER will not be mis-classified to other networks, but becomes non-classifiable at rate 0.0254. Overall, the classification error rates are quite low, so iPCR is proved working well.

A performance comparison between PCR and iPCR is shown in Fig. 5. In each subplot, in a unique network configuration, the green curve shows the true value (tVal) generated by simulation; the red dashed curve shows the predicted values by PCR; the black dotted curve represents the predicted results of iPCR. The shadow in the same color represents the range of standard deviation. As can be seen from the plots, the black curves are obviously closer to the green curves, better than the red curves, meaning that iPCR

TABLE 2: Confusion matrix of the CNN_c classifier for classifying unweighted networks. NC means the input is non-classifiable; (pre) represents the predicted type and (act) represents the actual type of the network.

	BA (pre)	ER (pre)	QSN (pre)	NW (pre)	NC
BA (act)	0.8333	0.0922	0	0	0.0745
ER (act)	0	0.9746	0	0	0.0254
QSN (act)	0	0.0165	0.9342	0	0.0494
NW (act)	0	0	0.0042	0.9833	0.0126

predicts the controllability more accurately than PCR, in all 12 cases. The results confirm that prior knowledge of the network topology is indeed helpful if correctly used. It is notable that the predicted curves are not as oscillatory as those obtained in [51], thanks to the filters used in both PCR and iPCR.

The average error calculated according to Eq. (4) is plotted in Fig. 6, where the black curve shows that iPCR has a lower average error (σ) than the red dashed curve of PCR, through the entire attacking process. The inset shows a clearer plot of the comparison for $P_N \in [0.9, 1]$. The average error is taken from all 12 configurations, namely, a total of 1200 testing samples. It is noticeable that both PCR and iPCR gain average errors with standard deviations much lower than that of the testing set (i.e., the 1200 testing samples), throughout the entire attack process.

4.3 Weighted Networks under Targeted Attacks

The controllability robustness prediction on weighted networks with size $N = 1000$ and average degree $\langle k \rangle \in [3, 5]$, under targeted node-removal attacks, is studied.

For each network instance, its average degree $\langle k \rangle$ is a real random number generated from the range of $[3, 5]$; its edge weights are uniformly-randomly assigned from the range of $(0, 1)$. Again, PCR contains a single CNN, while iPCR uses a CNN_{all} with four specialized CNN_{1,2,3,4} for the four types of networks respectively, if classifiable. The targeted attack performs node-removals according to the degrees of nodes, from high to low sequentially.

TABLE 3: Confusion matrix of the CNN_c classifier on classifying weighted networks. NC means the input is non-classifiable; (pre) represents the predicted type and (act) represents the actual type of the network; initial 'w' is for 'weighted'.

	wBA (pre)	wER (pre)	wQSN (pre)	wNW (pre)	UC
wBA (act)	0.9913	0	0	0	0.0087
wER (act)	0	0.9549	0.0150	0	0.0301
wQSN (act)	0	0	0.9915	0	0.0085
wNW (act)	0	0	0.0074	0.9815	0.0111

The confusion matrix shown in Table 3 suggests that the precision of the CNN_c classifier is high. Slightly dif-

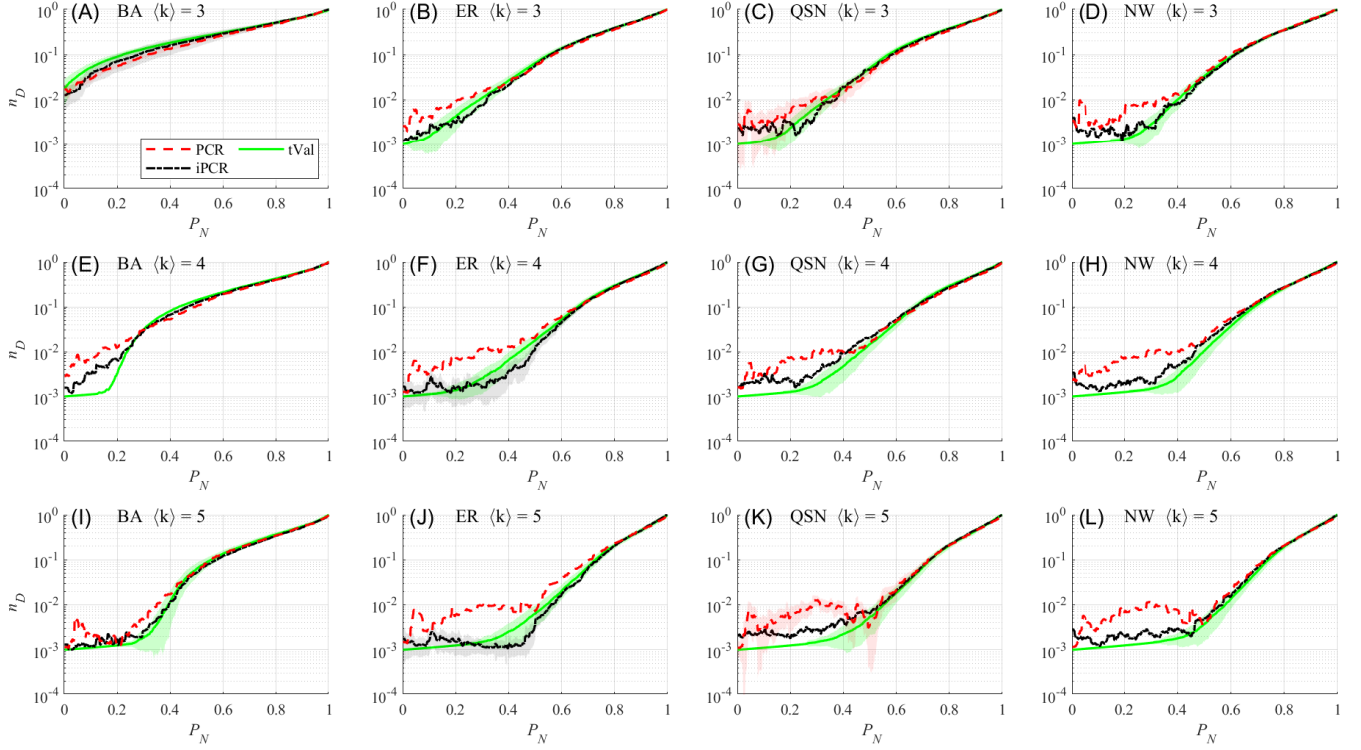


Fig. 5: [Color online] Comparison of PRC and iPCR on unweighted networks under random attacks. P_N represents the portion of nodes having been removed from the network; n_D is calculated by Eq. (1). Green curves: the true value (tVal) from simulation; red curves: predicted by PCR; black curves: predicted by iPCR. The shaded shadow in the same color represents the range of standard deviation.

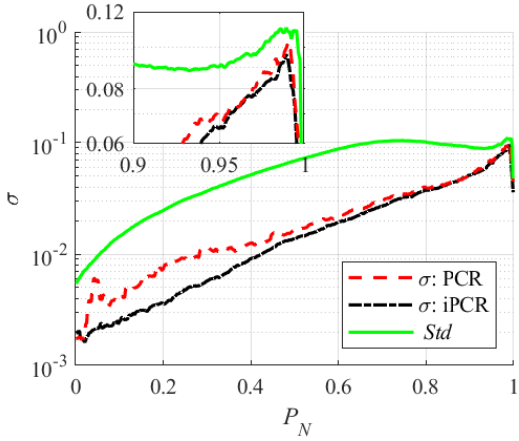


Fig. 6: [Color online] The average errors (σ) of PCR and iPCR. The inset gives a zoom-in picture for $P_N \in [0.9, 1]$. The green curve (Std) represents the standard deviation of the testing samples.

ferent from Table 2, here the CNN_c can either correctly classify the weighted BA and QSN respectively, or return a result of non-classifiable, without any mis-classification. The weighted ER and NW have very low probabilities to be classified as weighted QSN. Shuffling is also performed on these weighted networks. The overall precision on classifying weighted networks is slightly higher than that on unweighted networks.

In the experiments reported in Sec. 4.2, the average degree $\langle k \rangle$ is set to integers 3, 4, 5, respectively. Each column in Fig. 5 shows the same type of networks, with increasing $\langle k \rangle$ from 3 to 5. Although PCR and iPCR are trained without any information about the average degrees, as can be seen from Fig. 5, both PCR and iPCR return different predictions, when the input is of the same network type with different average degrees. However, this does not imply that average degree is a good feature or useful prior knowledge. In contrast, the average degree is known to be not suitable for preprocessing when used as prior knowledge. An example is given in the Supplementary Information (SI), where three network clusters are defined, namely ' $\langle k \rangle = 3$ ', ' $\langle k \rangle = 4$ ', and ' $\langle k \rangle = 5$ '. The prediction results is distorted due to the low precision of classification. This demonstrates that the prior knowledge used should be correct and appropriate, as common sense, otherwise misleading could happen.

Figure 7 shows the prediction results of PCR and iPCR on weighted networks under targeted attacks. Again, it is clear that, in each subplot, the black dotted curve is closer to the green curve than the red dashed curve. The higher precision of iPCR in prediction is partially due to the high classification rate presented in Table 3. Another reason is that an specialized CNN predictor is always better than a mixed one, as is intuitively so.

Figure 8 shows that the average prediction error of iPCR (black curve) is lower than that of PCR (red dashed curve), throughout the entire attack process. Note that both PCR and iPCR gain average errors with standard deviations

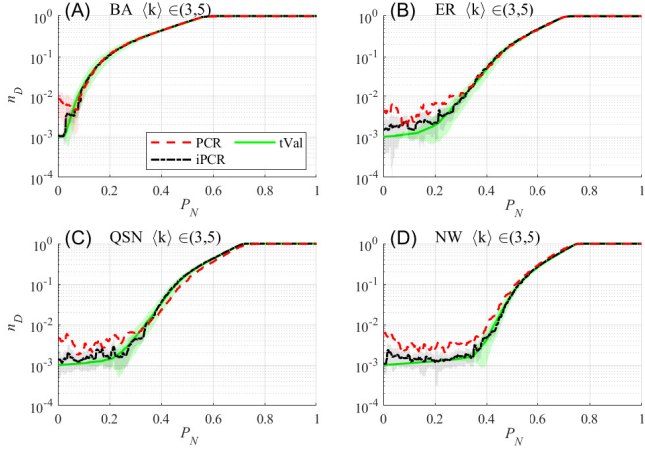


Fig. 7: [Color online] Comparison of PRC and iPCR on weighted networks under targeted attacks. P_N represents the portion of nodes having been removed from the network; n_D is calculated by Eq. (1). Green curves: the true value (tVal) from simulation; red curves: predicted by PCR; black curves: predicted by iPCR. The shaded shadow in the same color represents the range of standard deviation.

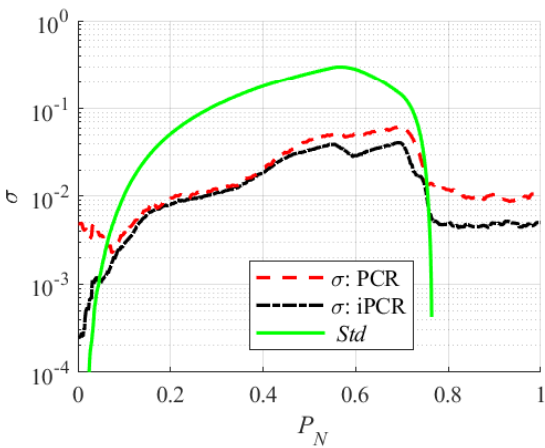


Fig. 8: [Color online] The average errors (σ) of PCR and iPCR. The green curve (Std) represents the standard deviation of the testing samples.

much lower than that of the testing samples through a long period. Differing from random attacks, in a targeted attack, when the portion of removed nodes is somewhat greater than 0.7, the network requires $n_D \approx 1$ to gain a full controllability. Although PCR and iPCR gain lower predictive errors during this stage (when P_N is somewhat greater than 0.7), the standard deviation of the testing sample actually becomes nearly zero.

4.4 Comparison of Prediction Measures

Spectral measures have long been used to quantify the *connectedness* robustness of complex networks against node- and edge-removal attacks. It has certain positive correlation to controllability, but they cannot be treated equally.

Here, six commonly-used spectral measures, namely spectral radius (SR), spectral gap (SG), natural connectiv-

ity (NCo), algebraic connectivity (ACo), effective resistance (ERe), and spanning tree count (STC) are compared in measuring the controllability robustness. Definitions and computational formulas for these measures can be found in, e.g., [29]. Recently, it was also found that heterogeneity (HE) reflects the controllability robustness [22]. In this paper, PCR and iPCR are used to predict the entire controllability curves in Secs. 4.2 and 4.3. Noticed that a predicted curve (a vector) can also be converted to a measure (a scalar) through Eq. (6). Thus, in the following, the above 9 prediction measures will be compared, namely, the 6 common spectral measures (SR, SG, NCo, ACo, ERe, STC), HE, PCR and iPCR.

The above prediction measures are used to predict the ordinal ranks of a total of 120 networks, for four network types with three different average degrees. These ranks are listed in a descending order in terms of controllability robustness, from the best to the worst. Specifically, each prediction measure returns a predicted rank list of the 120 networks. Then, the 9 rank lists returned by the 9 prediction measures are compared to the true rank list generated by simulation. The rank error information is summarized in Table 4, where the rank error σ_{rank} is calculated by

$$\sigma_{rank} = |rl_{pm} - rl_t|, \quad (12)$$

where rl_{pm} represents the rank list predicted by a prediction measure, and rl_t represents the true rank obtained from simulation.

For example, given two predicted rank lists, $rl_{pm1} = [3, 5, 2, 4, 1]$ and $rl_{pm2} = [1, 2, 4, 5, 3]$, and a true rank list, $rl_t = [1, 2, 3, 4, 5]$, the rank errors are obtained as $\sigma_{rank1} = [2, 3, 1, 0, 4]$, $\sigma_{rank2} = [1, 1, 1, 1, 2]$, respectively. The mean, maximum, and minimum of the rank error can be calculated accordingly. The number of '0' elements in a rank error list σ_{rank} is counted and then included in the 'correct rank' column. Finally, the number of networks, which includes the predicted top 10% and the confirmed top 10% by simulation, is counted and then included in the predicted 'top 10%' column. The number in the 'bot 10%' column is similarly calculated, where 'bot' is short for bottom. The detailed rank values of the 9 prediction measures are given in SI.

TABLE 4: Rank error information for the 9 predictive measures. Bold number means the best performing prediction measures.

	average rank error	max rank error	min rank error	correct rank	top 10%	bot 10%
SR	387.52	912	0	3	0	5
SG	370.09	933	1	0	0	7
NCo	394.58	993	0	3	0	5
ACo	496.98	1095	0	1	0	0
ERe	160.64	704	0	2	52	100
STC	547.14	1192	2	0	0	0
HE	187.13	910	0	2	13	91
PCR	112.72	481	0	2	46	104
iPCR	103.73	590	0	6	45	97

It can be seen from Table 4 that iPCR receives the minimum average rank error 103.73, followed by PCR. PCR obtains the minimum max rank error, followed by iPCR. Seven out of nine predictive measures receive a min rank error 0, meaning that these measures predict at least

one rank exactly as the true rank. iPCR predicts 6 ranks correctly. ERe predicts 52 top 10% networks that are truly 10% networks, although their exact ranks may be different, which are followed by PCR and iPCR that correctly predict 46 and 45 networks respectively. Finally, PRC well predicts 104 bottom 10% networks, followed by ERe and iPCR. The test dataset contains 1200 networks, hence there are 120 networks ranked as top and bottom 10%, respectively.

It is thus clear that PCR and iPCR return better prediction measures than the spectral measures and the heterogeneity. More importantly, PCR and iPCR return not only the predictive measures, but also the entire controllability changing process of a network against the node-removal attack; while the spectral measures and heterogeneity return only a single quantitative value for the controllability robustness.

However, it is notable that PCR and iPCR require a substantial amount of training data, while the spectral measures and heterogeneity do not. Nevertheless, as demonstrated in [51], the overhead in training a CNN is quite low which, compared to the exhaustive attack simulation, it is negligible.

5 CONCLUSIONS

Network controllability robustness, which reflects how well a networked system can maintain its controllability after destructive attacks, are usually measured via attack simulations. Such an exhaustive simulation approach can return the true value of the controllability robustness, but is computationally costly and very time consuming. The predictor of controllability robustness (PCR) employs a single convolutional neural network (CNN) to successfully achieve the prediction. In this paper, an improved multi-CNN and knowledge-based PCR (iPCR) is designed and evaluated, which takes advantage of prior knowledge from the given data. Extensive experimental studies, with thorough comparisons to eight other comparable measures, demonstrate that 1) the iPCR predicts more precisely than the PCR; 2) the iPCR provides a better predictive measure than the traditional spectral measures and network heterogeneity.

REFERENCES

- [1] A.-L. Barabási, *Network Science*. Cambridge University Press, 2016.
- [2] M. E. Newman, *Networks: An Introduction*. Oxford University Press, 2010.
- [3] G. Chen, X. Wang, and X. Li, *Fundamentals of Complex Networks: Models, Structures and Dynamics*, 2nd ed. John Wiley & Sons, 2014.
- [4] G. Chen and Y. Lou, *Naming Game: Models, Simulations and Analysis*. Springer, 2019.
- [5] Y.-Y. Liu, J.-J. Slotine, and A.-L. Barabási, "Controllability of complex networks," *Nature*, vol. 473, no. 7346, pp. 167–173, 2011.
- [6] Z. Z. Yuan, C. Zhao, Z. R. Di, W.-X. Wang, and Y.-C. Lai, "Exact controllability of complex networks," *Nature Communications*, vol. 4, p. 2447, 2013.
- [7] M. Pósfai, Y.-Y. Liu, J.-J. Slotine, and A.-L. Barabási, "Effect of correlations on network controllability," *Scientific Reports*, vol. 3, p. 1067, 2013.
- [8] G. Menichetti, L. Dall'Asta, and G. Bianconi, "Network controllability is determined by the density of low in-degree and out-degree nodes," *Physical Review Letters*, vol. 113, no. 7, p. 078701, 2014.
- [9] A. E. Motter, "Networkcontrology," *Chaos: An Interdisciplinary Journal of Nonlinear Science*, vol. 25, no. 9, p. 097621, 2015.
- [10] L. Wang, X. Wang, G. Chen, and W. K. S. Tang, "Controllability of networked mimo systems," *Automatica*, vol. 69, pp. 405–409, 2016.
- [11] Y.-Y. Liu and A.-L. Barabási, "Control principles of complex systems," *Review of Modern Physics*, vol. 88, no. 3, p. 035006, 2016.
- [12] L. Wang, X. Wang, and G. Chen, "Controllability of networked higher-dimensional systems with one-dimensional communication channels," *Royal Society Philosophical Transactions A*, vol. 375, no. 2088, p. 20160215, 2017.
- [13] L.-Z. Wang, Y.-Z. Chen, W.-X. Wang, and Y.-C. Lai, "Physical controllability of complex networks," *Scientific Reports*, vol. 7, p. 40198, 2017.
- [14] Y. Zhang and T. Zhou, "Controllability analysis for a networked dynamic system with autonomous subsystems," *IEEE Transactions on Automatic Control*, vol. 62, no. 7, pp. 3408–3415, 2016.
- [15] L. Xiang, F. Chen, W. Ren, and G. Chen, "Advances in network controllability," *IEEE Circuits and Systems Magazine*, vol. 19, no. 2, pp. 8–32, 2019.
- [16] Y.-Y. Liu, J.-J. Slotine, and A.-L. Barabási, "Control centrality and hierarchical structure in complex networks," *PLOS ONE*, vol. 7, no. 9, p. e44459, 2012.
- [17] E. Wu-Yan, R. F. Betzel, E. Tang, S. Gu, F. Pasqualetti, and D. S. Bassett, "Benchmarking measures of network controllability on canonical graph models," *Journal of Nonlinear Science*, pp. 1–39, 2018.
- [18] R. Zhang, X. Wang, M. Cheng, and T. Jia, "The evolution of network controllability in growing networks," *Physica A: Statistical Mechanics and its Applications*, vol. 520, pp. 257–266, 2019.
- [19] Y. Hao, Z. Duan, and G. Chen, "Further on the controllability of networked MIMO LTI systems," *International Journal of Robust and Nonlinear Control*, vol. 28, no. 5, pp. 1778–1788, 2018.
- [20] Y. Lou, L. Wang, and G. Chen, "Toward stronger robustness of network controllability: A snapback network model," *IEEE Transactions on Circuits and Systems I: Regular Papers*, vol. 65, no. 9, pp. 2983–2991, 2018.
- [21] G. Chen, Y. Lou, and L. Wang, "A comparative study on controllability robustness of complex networks," *IEEE Transactions on Circuits and Systems II: Express Briefs*, vol. 66, no. 5, pp. 828–832, 2019.
- [22] Y. Lou, L. Wang, and G. Chen, "Enhancing controllability robustness of q -snapback networks through redirecting edges," *Research*, vol. 2019, no. 7857534, 2019.
- [23] P. Holme, B. J. Kim, C. N. Yoon, and S. K. Han, "Attack vulnerability of complex networks," *Physical Review E*, vol. 65, no. 5, p. 056109, 2002.
- [24] B. Shargel, H. Sayama, I. R. Epstein, and Y. Bar-Yam, "Optimization of robustness and connectivity in complex networks," *Physical Review Letters*, vol. 90, no. 6, p. 068701, 2003.
- [25] C. M. Schneider, A. A. Moreira, J. S. Andrade, S. Havlin, and H. J. Herrmann, "Mitigation of malicious attacks on networks," *Proceedings of the National Academy of Sciences*, vol. 108, no. 10, pp. 3838–3841, 2011.
- [26] A. Bashan, Y. Berezin, S. Buldyrev, and S. Havlin, "The extreme vulnerability of interdependent spatially embedded networks," *Nature Physics*, vol. 9, pp. 667–672, 2013.
- [27] Y.-D. Xiao, S.-Y. Lao, L.-L. Hou, and L. Bai, "Optimization of robustness of network controllability against malicious attacks," *Chinese Physics B*, vol. 23, no. 11, p. 118902, 2014.
- [28] L. Bai, Y.-D. Xiao, L.-L. Hou, and S.-Y. Lao, "Smart rewiring: Improving network robustness faster," *Chinese Physics Letters*, vol. 32, no. 7, p. 078901, 2015.
- [29] H. Chan and L. Akoglu, "Optimizing network robustness by edge rewiring: A general framework," *Data Mining and Knowledge Discovery*, vol. 30, no. 5, pp. 1395–1425, 2016.
- [30] K. Yamashita, Y. Yasuda, R. Nakamura, and H. Ohsaki, "On the predictability of network robustness from spectral measures," in *2019 IEEE 43rd Annual Computer Software and Applications Conference (COMPSAC)*, vol. 2. IEEE, 2019, pp. 24–29.
- [31] L. Hou, S. Lao, B. Jiang, and L. Bai, "Enhancing complex network controllability by rewiring links," in *International Conference on Intelligent System Design and Engineering Applications (ISDEA)*. IEEE, 2013, pp. 709–711.
- [32] J. Xu, J. Wang, H. Zhao, and S. Jia, "Improving controllability of complex networks by rewiring links regularly," in *Chinese Control and Decision Conference (CCDC)*, 2014, pp. 642–645.

- [33] J. Liu, H. A. Abbass, and K. C. Tan, "Evolving robust networks using evolutionary algorithms," in *Evolutionary Computation and Complex Networks*. Springer, 2019, pp. 117–140.
- [34] S. Wang and J. Liu, "Designing comprehensively robust networks against intentional attacks and cascading failures," *Information Sciences*, vol. 478, pp. 125–140, 2019.
- [35] R. C. Gunasekara, C. K. Mohan, and K. Mehrotra, "Multi-objective optimization to improve robustness in networks," in *Multi-Objective Optimization*. Springer, 2018, pp. 115–139.
- [36] A. Zeng and W. Liu, "Enhancing network robustness against malicious attacks," *Physical Review E*, vol. 85, no. 6, p. 066130, 2012.
- [37] Z.-X. Wu and P. Holme, "Onion structure and network robustness," *Physical Review E*, vol. 84, no. 2, p. 026106, 2011.
- [38] T. Tanizawa, S. Havlin, and H. E. Stanley, "Robustness of onionlike correlated networks against targeted attacks," *Physical Review E*, vol. 85, no. 4, p. 046109, 2012.
- [39] Y. Hayashi and N. Uchiyama, "Onion-like networks are both robust and resilient," *Scientific Reports*, vol. 8, 2018.
- [40] L. Ma, J. Liu, and B. Duan, "Evolution of network robustness under continuous topological changes," *Physica A: Statistical Mechanics and its Applications*, vol. 451, pp. 623–631, 2016.
- [41] C.-L. Pu, W.-J. Pei, and A. Michaelson, "Robustness analysis of network controllability," *Physica A: Statistical Mechanics and its Applications*, vol. 391, no. 18, pp. 4420–4425, 2012.
- [42] X.-Y. Yan, W.-X. Wang, G. Chen, and D.-H. Shi, "Multiplex congruence network of natural numbers," *Scientific Reports*, vol. 6, p. 23714, 2016.
- [43] Y. Lou, L. Wang, K. F. Tsang, and G. Chen, "Towards optimal robustness of network controllability: An empirical necessary condition," *arXiv preprint:1912.12416*, 2019.
- [44] J. Schmidhuber, "Deep learning in neural networks: An overview," *Neural Networks*, vol. 61, pp. 85–117, 2015.
- [45] T. Wang, D. J. Wu, A. Coates, and A. Y. Ng, "End-to-end text recognition with convolutional neural networks," in *International Conference on Pattern Recognition (ICPR 2012)*. IEEE, 2012, pp. 3304–3308.
- [46] S. Lai, L. Xu, K. Liu, and J. Zhao, "Recurrent convolutional neural networks for text classification," in *AAAI Conference on Artificial Intelligence*, 2015, pp. 2267–2273.
- [47] X. Zhang, J. Zhao, and Y. LeCun, "Character-level convolutional networks for text classification," in *Advances in Neural Information Processing Systems (NIPS 2015)*, 2015, pp. 649–657.
- [48] H. Li, Z. Lin, X. Shen, J. Brandt, and G. Hua, "A convolutional neural network cascade for face detection," in *IEEE Conference on Computer Vision and Pattern Recognition (CVPR)*, 2015, pp. 5325–5334.
- [49] Y. Xiong, Y. Zhang, X. Kong, H. Chen, and Y. Zhu, "Graphinception: Convolutional neural networks for collective classification in heterogeneous information networks," *IEEE Transactions on Knowledge and Data Engineering*, 2019, doi:10.1109/TKDE.2019.2947458.
- [50] S. Du, T. Li, Y. Yang, and S.-J. Horng, "Deep air quality forecasting using hybrid deep learning framework," *IEEE Transactions on Knowledge and Data Engineering*, 2019, 10.1109/TKDE.2019.2954510.
- [51] Y. Lou, Y. He, L. Wang, and G. Chen, "Predicting network controllability robustness: A convolutional neural network approach," *arXiv preprint:1908.09471*, 2019.
- [52] J. Ruths and D. Ruths, "Robustness of network controllability under edge removal," in *Complex Networks IV*. Springer, 2013, pp. 185–193.
- [53] K. Simonyan and A. Zisserman, "Very deep convolutional networks for large-scale image recognition," *arXiv Preprint: 1409.1556*, 2014.
- [54] X. Glorot, A. Bordes, and Y. Bengio, "Deep sparse rectifier neural networks," in *International Conference on Artificial Intelligence and Statistics*, 2011, pp. 315–323.
- [55] C. M. Bishop, *Pattern Recognition and Machine Learning*. Springer, 2006.
- [56] A.-L. Barabási and R. Albert, "Emergence of scaling in random networks," *Science*, vol. 286, no. 5439, pp. 509–512, 1999.
- [57] P. Erdős and A. Rényi, "On the strength of connectedness of a random graph," *Acta Mathematica Hungarica*, vol. 12, no. 1-2, pp. 261–267, 1964.
- [58] M. E. Newman and D. J. Watts, "Renormalization group analysis of the small-world network model," *Physics Letters A*, vol. 263, no. 4-6, pp. 341–346, 1999.

Supplementary Information for the paper titled “Knowledge-Based Prediction of Network Controllability Robustness”

Yang Lou¹, Yaodong He¹, Lin Wang^{2,3}, Kim Fung Tsang¹, and Guanrong Chen * † ¹

¹Department of Electrical Engineering, City University of Hong Kong, Hong Kong, China

²Department of Automation, Shanghai Jiao Tong University, Shanghai 200240, China

³Key Laboratory of System Control and Information Processing, Ministry of Education, Shanghai 200240, China

1 An Example of Inappropriately Using Prior Knowledge

Table S1: Confusion matrix of the network classifier for classifying unweighted networks labeled by average degree. NC means the input is non-classifiable; (*pre*) represents the predicted type and (*act*) represents the actual type of the network.

	k_3 (<i>pre</i>)	k_4 (<i>pre</i>)	k_5 (<i>pre</i>)	NC
k_3 (<i>act</i>)	0.1270	0.0975	0	0.7755
k_4 (<i>act</i>)	0.0142	0.0438	0.0422	0.8998
k_5 (<i>act</i>)	0	0	0.6928	0.3072

Figure S1 show a comparison of PRC (predictor of controllability robustness) and iPCR_k (improved PCR; the subscript ‘k’ means using *average degree* as prior knowledge for classification) on predicting the controllability robustness of unweighted networks under random attacks.

PCR is trained and tested in the same way as it presented in the paper; while for iPCR_k, the average degree information is used as prior knowledge for classification. There are 3 clusters of networks, with $\langle k \rangle = 3$, $\langle k \rangle = 4$, and $\langle k \rangle = 5$, respectively.

As can be seen from Table S1, the average degree is a bad labeling method for the classifier, which cannot correctly classify different networks with different average degrees. In this case, iPCR_k has a higher probability to pass the input to a wrong predictor, thereby leading to a bad prediction. For example, a network with $\langle k \rangle = 3$ may be recognized as one with $\langle k \rangle = 4$, and then passed onto a classifier that was trained specifically using a substantial number of networks with $\langle k \rangle = 4$, but has never encountered any sample network with $\langle k \rangle = 3$ in training.

Due to the low precision in classification, the prediction results shown in Fig. S1 are expected to be unsatisfactory. A comparison of prediction errors is shown in Fig. S2. It is unexpected to see that the average error of iPCR_k is lower than PCR in the early stage, but becomes high in the late stage. However, when compared to the average error of iPCR, iPCR_k shows very imprecise performance in prediction, which is unsatisfactory overall. In conclusion, the average degree is a bad measure to use as prior knowledge for preprocessing.

*Corresponding author: Guanrong Chen (eegchen@cityu.edu.hk).

†Supported by the Hong Kong ITF Grant CityU ITP/058/17LP, the National Natural Science Foundation of China under Grant No. 61873167, and the Natural Science Foundation of Shanghai (No. 17ZR1445200).

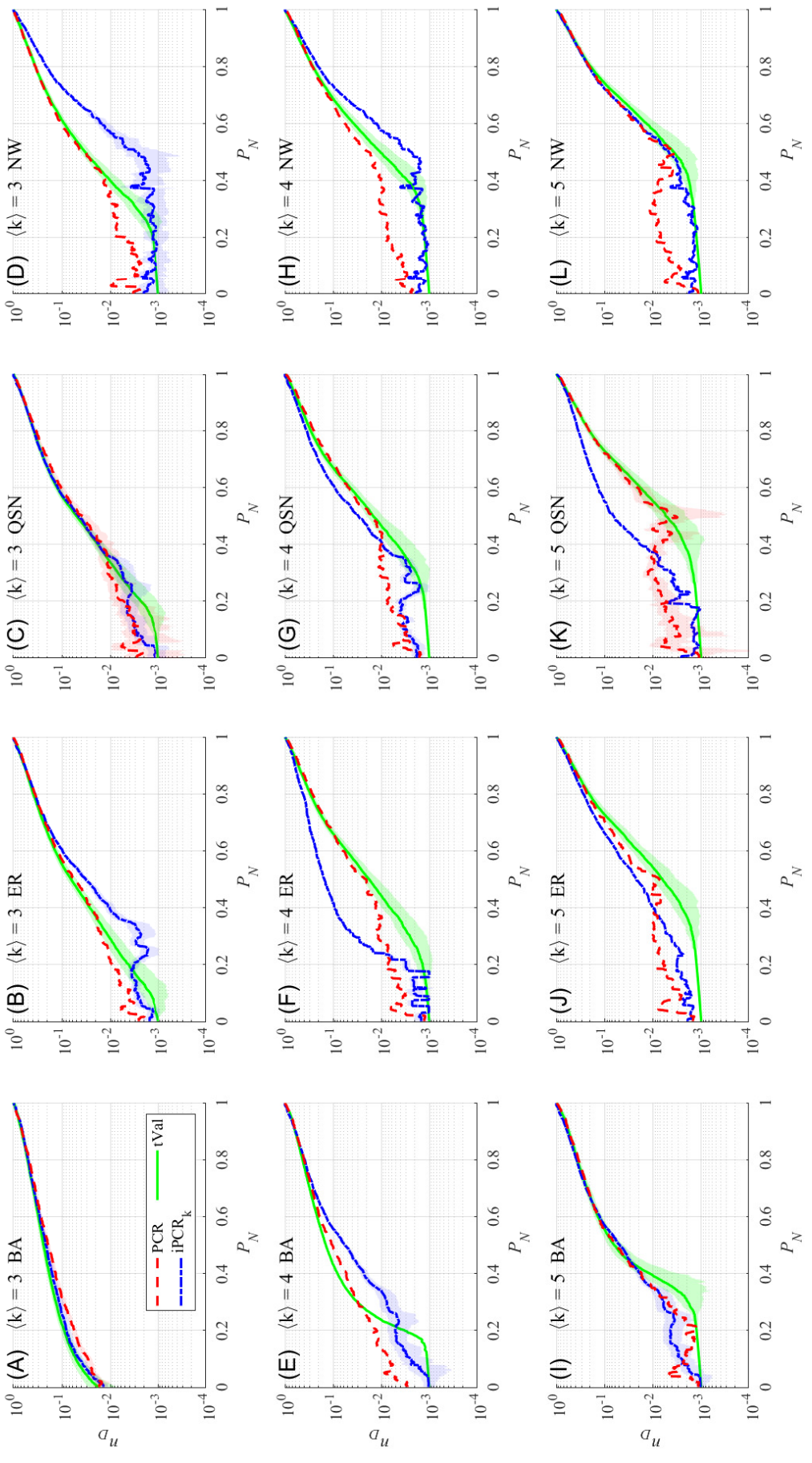


Figure S1: Comparison of PRC and iPCR on unweighted networks under random attacks. P_N represents the portion of nodes that have been removed from the network; n_D is the required density of the controlled nodes. Green curves: the true value (tVal) from simulation; red curves: predicted by PCR; black curves: predicted by iPCR. The shadow in the same color represents the range of standard deviation.

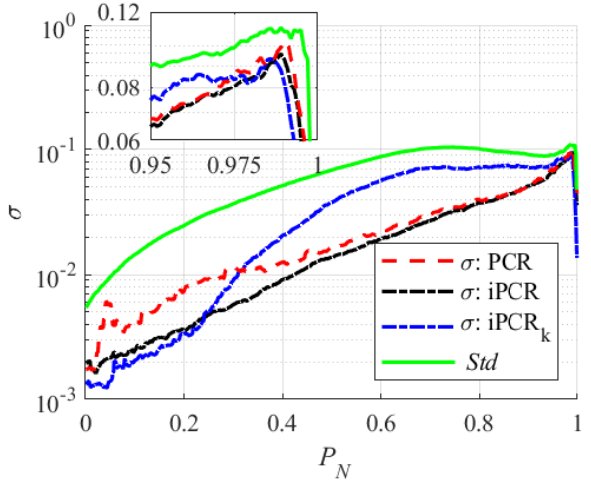


Figure S2: The average errors (σ) of PCR, iPCR, and $iPCR_k$. The green curve (Std) represents the standard deviation of the testing samples.

2 Detailed Ranks of Network Controllability

Tables S2–S31 show the detailed true ranks (tRank) and the ranks predicted by SR (spectral radius), SG (spectral gap), NCo (natural connectivity), ACo (algebraic connectivity), ERe (effective resistance), STC (spanning tree count), HE (heterogeneity), PCR, and iPCR, respectively. A bold italic number in the table indicates that the prediction measure predicts the true rank exactly.

Table S2: The true ranks (tRank) and the ranks predicted by SR (spectral radius), SG (spectral gap), NCo (natural connectivity), ACo (algebraic connectivity), ERe (effective resistance), STC (spanning tree count), HE (heterogeneity), PCR, and iPCR, respectively. [Part 1/30]

id	tRank	SR	SG	NCo	ACo	ERe	STC	HE	PCR	iPCR
1	1165	923	974	924	467	1139	164.5	1151	1124	1169
2	1133	902	949	902	489	1110	158	1007	1158	1015
3	1097	918	726	918	433	1154	42	1102	1187	1186
4	1172	925	734	925	402	1109	41	1106	1140	1175
5	1115	956	982	956	440	1170	33.5	1143	1134	1134
6	1135	910	964	910	428	1112	63	1020	1138	1146
7	1191	953	993	953	452	1148	19.5	1139	1168	1167
8	1160	957	984	957	436	1123	199	1137	1169	1198
9	1137	928	970	928	411	1135	63	1126	1125	1127
10	1200	980	1006	980	490	1192	8	1175	1176	1185
11	1189	936	975	936	464	1132	265.5	1109	1143	968
12	1127	929	728	929	430	1150	364.5	1145	1193	1174
13	1155	970	996	970	472	1155	281	1152	1133	1153
14	1139	989	736	989	407	1186	254.5	1191	1191	1142
15	1182	1000	745	1000	398	1169	46	1199	1197	1171
16	1130	921	979	921	383	1143	70.5	1119	1110	869
17	1114	931	969	931	482	1108	283	1089	1186	1180
18	1177	991	1015	991	427	1141	211	1194	1192	1199
19	1146	920	965	920	441	1114	25.5	1065	1152	1168
20	1178	961	1002	961	477	1183	191.5	1182	1184	1200
21	1175	995	744	995	438	1125	331.5	1198	1189	1196
22	1192	963	977	962	487	1184	33.5	1149	1113	1122
23	1142	965	1000	965	415	1120	154	1147	1180	1160
24	1195	908	952	908	475	1133	154	1079	1194	1144
25	1157	976	1012	976	417	1118	199	1167	1182	1164
26	1136	924	959	923	483	1121	161	1117	1156	1135
27	1196	962	1001	963	502	1171	206.5	1174	1122	1126
28	1143	949	987	950	404	1178	74.5	1158	1151	1136
29	1147	944	988	944	429	1165	25.5	1148	1177	1137
30	1166	903	951	903	391	1124	312	1048	1163	1159
31	1118	935	976	935	444	1160	209.5	1127	1162	1121
32	1156	979	742	979	422	1168	216.5	1179	1150	1119
33	1181	978	1010	978	474	1138	178.5	1173	1173	1193
34	1158	952	981	952	457	1167	114.5	1142	1160	1139
35	1194	994	741	994	468	1166	119	1192	1188	1149
36	1179	951	985	951	458	1157	139	1164	1147	1138
37	1163	996	1019	997	456	1182	80	1196	1136	1154
38	1129	927	962	927	455	1185	16	1131	1149	1176
39	1173	958	1011	958	478	1181	186	1153	1111	1150
40	1125	941	986	941	408	1152	147.5	1146	1135	1157

Table S3: The true ranks (tRank) and the ranks predicted by SR (spectral radius), SG (spectral gap), NCo (natural connectivity), ACo (algebraic connectivity), ERe (effective resistance), STC (spanning tree count), HE (heterogeneity), PCR, and iPCR, respectively. [Part 2/30]

id	tRank	SR	SG	NCo	ACo	ERe	STC	HE	PCR	iPCR
41	1148	946	978	946	409	1101	261.5	1091	1102	1020
42	1161	988	1014	988	434	1137	269	1186	1159	1120
43	1132	997	1016	996	496	1197	9	1190	1196	1148
44	1170	926	967	926	442	1198	67	1111	1129	1197
45	1153	906	950	906	446	1175	38	1040	1121	1141
46	1105	912	966	912	486	1115	300	1074	1171	1140
47	1144	933	980	933	488	1140	199	1116	1103	1005
48	1120	922	961	922	437	1149	103	1136	1185	1183
49	1198	915	955	915	399	1144	194.5	1138	1137	964
50	1174	973	1005	972	443	1156	203	1171	1179	1162
51	1145	984	1018	984	425	1142	139	1178	1181	1131
52	1100	916	956	916	465	1107	81	1024	1120	1118
53	1123	934	973	934	450	1117	59	1122	1116	1117
54	1185	968	992	968	471	1130	55	1155	1130	1194
55	1106	987	1017	987	431	1134	312	1176	1112	1032
56	1109	904	727	904	448	1105	254.5	1047	1199	1191
57	1126	959	729	959	414	1119	232.5	1172	1198	1188
58	1180	955	743	955	426	1153	122.5	1140	1132	1133
59	1188	939	990	939	379	1146	281	1110	1144	1170
60	1131	907	958	907	418	1151	272.5	1068	1190	1177
61	1193	975	1008	975	463	1180	178.5	1187	1105	1172
62	1128	993	1022	993	462	1158	168.5	1188	1153	1147
63	1150	999	1027	999	476	1176	173.5	1200	1170	1156
64	1149	971	1007	971	492	1163	399	1166	1165	1124
65	1122	940	739	940	453	1106	373	1107	1161	1125
66	1134	930	733	930	466	1128	249	1124	1172	1123
67	1190	937	732	937	405	1173	122.5	1168	1195	1178
68	1112	998	1028	998	481	1131	70.5	1195	1118	1151
69	1111	954	730	954	445	1196	356.5	1160	1167	1128
70	1117	943	994	943	473	1111	151	1133	1119	1195
71	1164	905	947	905	416	1102	168.5	1011	1127	1166
72	1141	964	1003	964	435	1194	37	1163	1178	1158
73	1138	974	735	974	480	1190	216.5	1185	1104	996
74	1108	950	997	949	439	1122	147.5	1144	1146	1145
75	1140	945	1004	945	461	1127	315.5	1159	1148	1019
76	1107	967	989	967	424	1177	319	1157	1157	1189
77	1119	966	983	966	410	1193	67	1165	1106	1116
78	1183	932	960	932	470	1191	139	1130	1164	1184
79	1154	909	954	909	469	1103	76	1032	1108	1161
80	1124	982	731	982	494	1188	220.5	1189	1131	1165

Table S4: The true ranks (tRank) and the ranks predicted by SR (spectral radius), SG (spectral gap), NCo (natural connectivity), ACo (algebraic connectivity), ERe (effective resistance), STC (spanning tree count), HE (heterogeneity), PCR, and iPCR, respectively. [Part 3/30]

id	tRank	SR	SG	NCo	ACo	ERe	STC	HE	PCR	iPCR
81	1110	990	1020	990	432	1172	206.5	1180	1155	1163
82	1116	986	1023	986	499	1187	91.5	1197	1115	974
83	1197	977	999	977	423	1200	127.5	1181	1200	1192
84	1171	917	968	917	504	1164	35.5	1084	1174	1173
85	1152	919	957	919	449	1136	212	1096	1154	1187
86	1094	985	1009	985	459	1174	55	1177	1107	1152
87	1169	969	998	969	485	1162	206.5	1154	1114	989
88	1186	992	1013	992	491	1189	147.5	1184	1100	955
89	1113	981	995	981	388	1199	73	1170	1139	1155
90	1121	913	963	913	400	1116	277	1082	1166	1129
91	1167	972	725	973	395	1145	364.5	1193	1183	1190
92	1168	983	1021	983	501	1147	147.5	1183	1123	988
93	1184	948	738	948	460	1179	242	1162	1109	1000
94	1187	914	953	914	412	1126	261.5	1073	1141	1182
95	1151	938	991	938	484	1195	133.5	1161	1145	1024
96	1159	942	972	942	403	1113	203	1118	1128	1179
97	1199	947	737	947	397	1159	104	1169	1175	1143
98	1176	960	740	960	421	1129	216.5	1156	1142	1132
99	1162	901	948	901	401	1161	59	990	1117	1130
100	1103	911	971	911	454	1104	173.5	1059	1126	1181
101	893	1031	748	1031	838	761	644	1021	1043	1042
102	1058	1056	750	1056	839	765	435	1076	1084	1115
103	1089	1054	1093	1054	909	751	687	1057	1064	683
104	1004	1037	1072	1037	862	733	701	1061	1007	1067
105	1009	1042	1056	1042	889	714	694	1006	988	639
106	1029	1008	1031	1008	874	750	485	944	1042	1110
107	1068	1046	1073	1046	834	713	547.5	1004	1028	1076
108	896	1004	1025	1004	880	701	554.5	916	1030	1033
109	1038	1088	1100	1088	903	791	590	1120	1015	544
110	1065	1079	759	1079	899	769	558	1083	1054	1066
111	1090	1092	758	1092	879	794	482	1123	1094	1106
112	1070	1094	1107	1094	852	756	632.5	1128	1020	999
113	1093	1018	752	1018	912	799	747.5	1086	1029	1069
114	1030	1036	1059	1036	858	721	504.5	1071	1025	1080
115	1067	1009	1030	1009	819	744	545.5	974	1012	1083
116	1018	1023	1061	1023	825	718	599.5	1017	956	967
117	1035	1059	1087	1059	806	762	475.5	1036	1096	1025
118	1042	1061	1088	1061	813	795	407.5	1092	1045	1087
119	1028	1071	1090	1071	869	727	493	1042	1047	1047
120	1061	1068	1101	1068	847	788	537	1093	1033	1043

Table S5: The true ranks (tRank) and the ranks predicted by SR (spectral radius), SG (spectral gap), NCo (natural connectivity), ACo (algebraic connectivity), ERe (effective resistance), STC (spanning tree count), HE (heterogeneity), PCR, and iPCR, respectively. [Part 4/30]

id	tRank	SR	SG	NCo	ACo	ERe	STC	HE	PCR	iPCR
121	1048	1086	1079	1086	911	754	428	1135	1057	1075
122	1041	1060	1069	1060	870	755	638.5	1069	1085	584
123	1034	1066	1071	1065	860	729	413	1056	925	1041
124	1008	1012	756	1012	906	790	753.5	1001	1081	1103
125	1036	1033	1045	1033	872	764	553	1052	1072	1070
126	815	1055	1066	1055	898	720	537	1037	1073	1077
127	1033	1011	1042	1011	904	728	575.5	967	1083	1022
128	1055	1089	1089	1089	884	724	473.5	1105	1082	1030
129	1076	1017	1032	1017	850	723	694	1035	1074	1085
130	1044	1001	746	1001	890	707	769	908	1093	1035
131	986	1003	1026	1003	818	748	412	923	999	1027
132	1104	1082	1106	1082	855	776	402	1099	1079	613
133	1072	1100	1109	1100	915	800	422	1150	1009	1065
134	1031	1047	1048	1047	823	702	521	998	986	1094
135	1039	1034	1074	1034	849	784	429	1014	955	1089
136	1025	1075	1091	1075	835	785	442	1098	1058	1063
137	1043	1090	760	1090	851	739	738.5	1103	1077	1079
138	875	1002	1024	1002	821	708	632.5	917	1088	802
139	1037	1043	1057	1043	864	777	593.5	1051	950	1100
140	1046	1096	1092	1096	841	767	570	1125	1098	1073
141	1021	1069	1064	1069	837	732	702	1078	995	1045
142	1077	1029	1086	1029	820	725	433	1038	1086	973
143	1040	1080	1085	1080	845	786	469	1114	1035	1054
144	1102	1062	1083	1062	892	792	415	1094	974	1102
145	1032	1026	1050	1026	828	709	699.5	1026	1099	1051
146	972	1021	1053	1022	830	703	717.5	993	1062	1068
147	1079	1058	1076	1058	891	753	537	1041	1069	1059
148	897	1039	1051	1039	883	737	515.5	1060	1008	1082
149	991	1035	1047	1035	848	793	498.5	1070	1017	1071
150	1078	1051	1055	1051	876	741	697	1050	1031	1105
151	1087	1045	1063	1045	885	783	454.5	1044	1087	1098
152	1099	1077	1081	1077	887	735	697	1072	1010	1114
153	1000	1005	1036	1005	910	749	713.5	1000	1052	1031
154	928	1007	1039	1007	826	717	462.5	926	1046	1060
155	1045	1098	1104	1098	843	773	403	1141	1037	1074
156	963	1093	1105	1093	831	740	475.5	1112	1091	1040
157	1073	1070	1078	1070	908	796	552	1095	1101	1018
158	1083	1030	751	1030	877	719	687	1012	1075	1055
159	1069	1057	1060	1057	902	758	444	1034	1050	1061
160	1095	1065	1068	1066	865	726	628.5	1077	1071	686

Table S6: The true ranks (tRank) and the ranks predicted by SR (spectral radius), SG (spectral gap), NCo (natural connectivity), ACo (algebraic connectivity), ERe (effective resistance), STC (spanning tree count), HE (heterogeneity), PCR, and iPCR, respectively. [Part 5/30]

id	tRank	SR	SG	NCo	ACo	ERe	STC	HE	PCR	iPCR
161	1060	1083	1097	1083	833	763	447.5	1100	1019	936
162	996	1074	1094	1074	846	772	691	1101	1078	1064
163	1050	1049	1049	1049	871	734	784	1058	1032	1037
164	1019	1073	1075	1073	896	747	597	1113	1092	1057
165	1063	1091	749	1091	882	766	659.5	1132	1076	1039
166	1092	1085	1084	1085	881	722	515.5	1064	1090	980
167	1085	1022	1037	1021	907	770	592	1025	1022	1072
168	1051	1010	1035	1010	854	771	599.5	1008	1048	1048
169	1024	1019	757	1019	863	746	762	982	1066	1062
170	1064	1041	1062	1041	894	738	527.5	1031	1036	1046
171	1096	1064	1070	1064	893	789	728	1080	1013	1113
172	1098	1016	1043	1016	888	711	640	1009	1070	1107
173	1057	1006	747	1006	905	710	668.5	918	1000	1097
174	1054	1078	1082	1078	875	782	537	1085	1051	1044
175	946	1038	1054	1038	897	745	511	1027	1041	1084
176	1049	1097	1102	1097	810	768	450	1115	1065	1090
177	1053	1013	755	1013	867	715	684.5	955	1063	1056
178	1088	1087	1095	1087	844	757	727	1129	1097	1111
179	1075	1032	1046	1032	816	716	416.5	1066	1067	1093
180	890	1020	1034	1020	901	743	615.5	1022	1027	1088
181	1052	1063	754	1063	916	798	652	1097	1095	1038
182	1059	1081	1096	1081	822	730	470	1104	1053	1108
183	1066	1072	1108	1072	814	774	462.5	1088	1023	1109
184	1086	1024	753	1024	827	712	678	996	998	1092
185	1047	1076	1098	1076	913	742	632.5	1090	1068	1101
186	1091	1044	1058	1044	829	704	508	980	996	1099
187	1062	1095	1103	1095	868	797	585	1121	1055	1081
188	1080	1028	1040	1028	842	736	423	1033	1024	1058
189	964	1040	1044	1040	836	781	556	1081	1002	1078
190	1081	1099	1110	1099	856	787	504.5	1134	1034	1112
191	1071	1014	1029	1014	861	731	720.5	979	989	1049
192	1082	1025	1033	1025	857	780	431	972	1061	1095
193	1056	1052	1067	1052	866	760	466.5	1055	1056	1050
194	1084	1027	1038	1027	873	759	513	984	1060	1052
195	1014	1053	1077	1053	886	705	420	981	1059	1096
196	1074	1084	1099	1084	859	778	549.5	1108	1080	1091
197	1101	1050	1065	1050	878	779	603.5	1054	1044	1104
198	1026	1067	1080	1067	840	706	444	1039	1089	1053
199	894	1048	1052	1048	817	775	416.5	1049	1039	827
200	957	1015	1041	1015	895	752	613	983	1016	1086

Table S7: The true ranks (tRank) and the ranks predicted by SR (spectral radius), SG (spectral gap), NCo (natural connectivity), ACo (algebraic connectivity), ERe (effective resistance), STC (spanning tree count), HE (heterogeneity), PCR, and iPCR, respectively. [Part 6/30]

id	tRank	SR	SG	NCo	ACo	ERe	STC	HE	PCR	iPCR
201	838	1182	1179	1182	1179	376	840	1046	625	646
202	743	1138	1156	1138	1143	371	1038.5	947	882	781
203	629	1137	1138	1137	1129	321	1038.5	934	666	607
204	783	1115	1121	1115	1101	374	991	929	686	743
205	713	1193	770	1193	1193	339	921.5	1018	959	822
206	834	1166	1194	1166	1117	369	1074	1005	603	622
207	852	1149	769	1149	1182	386	1002	986	621	663
208	984	1106	1115	1106	1135	347	806	909	693	629
209	851	1125	1132	1125	1185	388	808	935	609	618
210	955	1129	1130	1129	1113	319	858.5	932	634	878
211	709	1163	1165	1163	1115	392	897	999	773	739
212	429	1180	1170	1180	1175	348	834.5	994	640	897
213	574	1151	1144	1151	1196	365	822.5	943	709	713
214	877	1186	1195	1186	1158	381	1077	1045	1014	920
215	720	1178	1184	1178	1166	399	1136	1010	952	899
216	705	1173	1183	1173	1109	305	850.5	971	883	724
217	656	1158	765	1158	1138	322	1008.5	995	1049	824
218	519	1114	1129	1114	1163	340	946	939	934	545
219	959	1172	1177	1172	1177	341	1049.5	976	994	826
220	760	1102	1113	1102	1159	304	890.5	903	681	656
221	701	1192	1190	1192	1181	379	973	1043	697	761
222	584	1160	1148	1160	1192	324	1038.5	952	725	698
223	722	1191	1185	1191	1131	390	803	1029	760	771
224	934	1199	1198	1199	1147	364	850.5	1075	653	611
225	554	1127	1136	1127	1116	338	911.5	910	626	680
226	749	1196	1186	1196	1191	361	1075.5	1063	903	865
227	1013	1105	1116	1105	1194	309	1158	905	954	888
228	628	1200	1197	1200	1122	363	1042.5	1067	915	747
229	631	1131	1151	1131	1195	301	1144.5	945	698	742
230	819	1156	762	1156	1119	352	1107.5	969	1021	911
231	913	1153	1158	1153	1153	366	1196	975	636	665
232	735	1155	761	1155	1136	362	1182	1002	885	835
233	757	1189	1178	1189	1171	337	860.5	1019	818	699
234	583	1132	1150	1132	1188	355	1141.5	950	944	715
235	994	1167	1191	1167	1139	346	1051.5	989	783	798
236	777	1175	1175	1175	1176	375	968	1016	721	685
237	669	1136	1128	1136	1160	306	881	914	607	623
238	872	1161	764	1161	1141	382	906	959	642	608
239	798	1111	763	1111	1123	315	1117	925	858	729
240	616	1165	1169	1165	1132	377	1051.5	985	895	675

Table S8: The true ranks (tRank) and the ranks predicted by SR (spectral radius), SG (spectral gap), NCo (natural connectivity), ACo (algebraic connectivity), ERe (effective resistance), STC (spanning tree count), HE (heterogeneity), PCR, and iPCR, respectively. [Part 7/30]

id	tRank	SR	SG	NCo	ACo	ERe	STC	HE	PCR	iPCR
241	782	1144	1153	1144	1148	360	911.5	927	822	859
242	662	1152	1155	1152	1127	318	868.5	933	717	762
243	967	1112	766	1112	1173	344	1071.5	913	718	741
244	675	1121	1143	1121	1161	370	1138.5	928	637	657
245	661	1117	1154	1117	1154	393	863	930	889	601
246	726	1190	1187	1190	1118	330	894	1028	598	432
247	906	1181	1168	1181	1172	394	888	978	615	661
248	813	1142	1142	1142	1168	333	1141.5	938	962	760
249	601	1157	1163	1157	1183	327	1125.5	960	645	673
250	738	1150	1161	1150	1085	397	830.5	997	618	637
251	974	1162	1164	1162	1164	323	1194	966	643	674
252	883	1164	1160	1164	1189	378	801	964	592	707
253	692	1119	1118	1119	1197	311	1024.5	922	579	296
254	646	1128	1134	1128	1099	343	885.5	940	614	777
255	776	1123	1131	1123	1121	314	1146	920	1018	894
256	746	1174	1180	1174	1104	310	809	963	701	664
257	570	1135	1135	1135	1124	329	825	953	654	1007
258	708	1183	1181	1183	1199	396	847.5	1013	808	718
259	740	1171	1167	1171	1137	385	976.5	992	646	643
260	930	1113	1122	1113	1112	308	1075.5	915	658	694
261	927	1107	1125	1107	1108	302	1032	906	971	807
262	773	1134	1123	1134	1155	373	1016	956	784	684
263	621	1170	1174	1170	1146	345	940	965	793	748
264	786	1147	1159	1147	1151	351	991	977	985	727
265	647	1139	1162	1139	1134	303	1136	936	867	751
266	533	1159	1140	1159	1187	380	995	949	710	767
267	827	1122	1147	1122	1128	398	817.5	951	613	403
268	731	1108	1117	1108	1184	342	870	907	641	636
269	853	1185	767	1185	1174	389	994	1030	977	668
270	945	1179	1171	1179	1165	316	1066	957	781	355
271	779	1194	1193	1194	1133	353	805	991	841	877
272	998	1177	1188	1177	1110	357	827	1015	667	735
273	1020	1146	768	1146	1111	332	1111.5	962	942	752
274	685	1103	1112	1103	1106	320	942.5	902	727	455
275	950	1140	1120	1140	1126	391	917	961	970	734
276	686	1109	1126	1109	1150	313	888	912	993	720
277	747	1116	1127	1116	1140	356	1197.5	931	583	645
278	651	1118	1133	1118	1120	383	985.5	958	941	765
279	962	1154	1146	1154	1142	307	819	921	699	702
280	657	1169	1157	1169	1092	326	1019.5	973	931	763

Table S9: The true ranks (tRank) and the ranks predicted by SR (spectral radius), SG (spectral gap), NCo (natural connectivity), ACo (algebraic connectivity), ERe (effective resistance), STC (spanning tree count), HE (heterogeneity), PCR, and iPCR, respectively. [Part 8/30]

id	tRank	SR	SG	NCo	ACo	ERe	STC	HE	PCR	iPCR
281	889	1176	1182	1176	1125	317	983	970	1006	823
282	925	1168	1176	1168	1186	335	1144.5	987	659	695
283	666	1143	1152	1143	1105	384	1141.5	968	648	778
284	754	1184	1192	1184	1156	336	816	1003	795	839
285	689	1145	1139	1145	1102	350	883.5	954	973	820
286	859	1101	1111	1101	1190	328	1066	901	916	821
287	884	1188	1189	1188	1145	367	890.5	988	628	653
288	975	1198	1199	1198	1114	400	961	1087	692	692
289	990	1124	1141	1124	1152	358	901.5	946	747	942
290	829	1104	1114	1104	1198	349	1042.5	904	1003	921
291	916	1195	1196	1195	1180	372	1134	1053	682	655
292	755	1120	1124	1120	1144	312	908.5	919	587	582
293	973	1197	1200	1197	1170	395	1158	1062	1026	916
294	653	1130	1145	1130	1178	354	1154.5	942	948	726
295	639	1126	1137	1126	1167	325	830.5	924	981	805
296	753	1133	1149	1133	1162	368	980	937	612	696
297	846	1141	1166	1141	1157	331	847.5	941	616	452
298	699	1110	1119	1110	1107	334	860.5	911	672	310
299	915	1148	1172	1148	1130	359	830.5	948	715	625
300	625	1187	1173	1187	1169	387	915.5	1023	711	693
301	866	292	232	169	10	1091	386	887	938	1010
302	805	251	180	155	134	1078	356.5	857	983	1009
303	924	221	217	121	94	983	341.5	810	992	995
304	937	273	202	160	168	1070	389.5	860	890	845
305	873	238	107	131	36	1061	327	829	884	794
306	882	299	131	188	170	1053	347	883	966	990
307	954	227	153	124	202	1019	249	818	811	940
308	989	229	156	148	15	1092	242	827.5	845	1013
309	1010	258	195	177	139	1058	249	869	893	1008
310	988	236	243	140	81	1049	220.5	836	866	981
311	1016	293	241	184	152	1071	386	891	899	892
312	920	295	152	192	56	1094	328.5	899	778	970
313	1002	240	207	115	101	1001	347	833	907	963
314	918	291	129	178	162	1017	341.5	884	888	991
315	942	270	233	181	48	993	44	838.5	980	953
316	895	234	246	136	66	1032	122.5	821	662	962
317	849	283	191	182	61	1057	391.5	888	806	876
318	976	260	245	144	153	1035	373	850	700	868
319	983	246	166	168	39	1073	242	853.5	807	1002
320	912	266	248	159	272	918	373	867	819	913

Table S10: The true ranks (tRank) and the ranks predicted by SR (spectral radius), SG (spectral gap), NCo (natural connectivity), ACo (algebraic connectivity), ERe (effective resistance), STC (spanning tree count), HE (heterogeneity), PCR, and iPCR, respectively. [Part 9/30]

id	tRank	SR	SG	NCo	ACo	ERe	STC	HE	PCR	iPCR
321	679	289	206	199	69	1056	242	898	968	1016
322	850	242	201	126	143	999	232.5	827.5	871	951
323	1007	200	112	110	175	921	254.5	810	758	893
324	857	217	171	162	33	1080	214	849	978	902
325	902	199	818	100	144	931	288.5	805	887	918
326	712	255	240	175	216	1034	331.5	847	979	1036
327	792	277	820	191	116	1072	79	897	920	874
328	931	241	224	138	12	1082	254.5	835	924	983
329	870	249	817	157	192	1044	296.5	848	825	957
330	688	296	172	196	154	1098	229.5	896	951	950
331	898	224	239	119	5	1028	356.5	840	917	987
332	793	210	213	97	155	1037	236	802	840	1026
333	868	254	813	156	7	1067	293	861	687	1011
334	985	275	220	170	20	1099	335.5	874	975	854
335	980	235	205	130	115	938	341.5	837	674	923
336	1027	267	203	185	172	1069	39	873	759	812
337	965	269	179	150	80	1033	373	842	1011	1006
338	903	233	157	147	188	970	110.5	823	929	901
339	844	276	222	167	18	1083	364.5	858.5	651	678
340	891	253	148	161	283	990	394	851	854	1003
341	640	228	210	123	82	1065	308.5	816	891	837
342	1003	285	225	190	208	1041	335.5	889.5	894	965
343	796	259	223	152	128	1023	269	846	963	932
344	977	247	244	142	93	1050	364.5	845	827	977
345	697	294	139	197	25	1085	380.5	900	987	882
346	751	222	209	128	24	1084	373	864	1001	887
347	961	187	185	107	249	903	119	812	730	797
348	952	226	236	132	190	1048	113	825	902	926
349	737	282	189	187	176	1063	335.5	892	964	944
350	1001	265	231	164	1	1089	224	871	879	1017
351	848	208	159	117	3	1051	229.5	808	947	1028
352	901	232	165	129	210	939	351	815	824	986
353	867	245	238	153	86	1076	396	878	965	998
354	800	219	208	125	157	1005	226.5	813	805	979
355	719	209	216	99	219	907	380.5	804	864	966
356	1023	279	250	173	54	1097	356.5	893	901	994
357	887	284	186	195	45	1096	144	895	957	938
358	971	290	132	166	57	1059	373	881	949	971
359	789	230	218	120	185	942	323	814	844	972
360	982	220	235	135	113	1046	242	843.5	847	937

Table S11: The true ranks (tRank) and the ranks predicted by SR (spectral radius), SG (spectral gap), NCo (natural connectivity), ACo (algebraic connectivity), ERe (effective resistance), STC (spanning tree count), HE (heterogeneity), PCR, and iPCR, respectively. [Part 10/30]

id	tRank	SR	SG	NCo	ACo	ERe	STC	HE	PCR	iPCR
361	914	263	158	146	19	1038	351	841	738	873
362	729	272	237	189	51	1090	249	885.5	849	1001
363	939	237	198	127	44	998	335.5	830.5	874	992
364	911	204	221	112	169	991	242	826	719	924
365	943	243	197	139	187	1030	341.5	855	788	931
366	905	274	242	176	71	984	347	870	976	976
367	921	214	229	118	76	1060	341.5	820	997	833
368	1011	211	199	102	232	910	373	803	870	978
369	929	271	169	172	214	1043	328.5	858.5	669	939
370	948	280	135	194	58	1075	23	881	940	922
371	951	252	145	158	87	1054	347	865	991	982
372	659	278	234	171	111	1093	341.5	881	900	946
373	1017	262	196	163	173	1066	325	866	728	1004
374	956	250	176	154	171	1000	356.5	853.5	828	810
375	830	281	219	183	17	1100	199	868	984	927
376	960	264	227	180	136	1081	257.5	879	1040	1034
377	949	256	204	141	167	1039	322	834	880	1014
378	824	244	228	143	226	1047	356.5	872	908	896
379	936	216	212	108	161	1007	338	822	990	956
380	981	206	144	109	243	905	386	817	886	917
381	840	203	122	116	85	1055	391.5	810	713	934
382	756	218	200	134	147	1040	394	838.5	877	1023
383	762	248	147	151	21	1095	356.5	862	919	1012
384	806	286	174	186	27	1086	119	877	816	1029
385	947	298	177	198	9	1079	224	894	927	975
386	791	268	140	165	148	986	356.5	852	860	928
387	910	205	102	103	14	901	317	801	843	969
388	941	239	162	137	42	1077	249	819	913	952
389	938	225	164	122	13	1020	380.5	843.5	780	909
390	809	297	163	200	92	1074	259	885.5	754	905
391	842	195	151	111	127	922	380.5	806	904	941
392	752	287	230	174	178	1068	229.5	889.5	706	997
393	997	231	154	133	119	1064	108.5	824	839	915
394	765	261	190	145	68	1031	364.5	863	1038	985
395	900	213	215	104	183	1027	380.5	807	953	1021
396	843	257	247	149	35	1062	364.5	856	853	929
397	923	288	214	179	255	943	236	875	863	993
398	966	223	149	114	8	1087	398	832	982	961
399	804	215	188	113	50	996	286	830.5	1005	861
400	839	300	249	193	11	1088	105	876	928	791

Table S12: The true ranks (tRank) and the ranks predicted by SR (spectral radius), SG (spectral gap), NCo (natural connectivity), ACo (algebraic connectivity), ERe (effective resistance), STC (spanning tree count), HE (heterogeneity), PCR, and iPCR, respectively. [Part 11/30]

id	tRank	SR	SG	NCo	ACo	ERe	STC	HE	PCR	iPCR
401	433	484	450	378	517	613	647.5	593	516	335
402	466	564	464	473	324	686	557	714	442	404
403	545	576	442	481	237	664	681.5	733	384	468
404	500	527	376	439	653	597	673	662	418	408
405	411	496	378	390	635	601	762	598.5	441	356
406	304	580	473	482	593	629	653	750.5	599	597
407	422	568	431	466	633	666	791	704.5	414	469
408	194	587	440	485	102	683	642	737	544	383
409	404	556	467	452	509	644	742.5	681.5	510	451
410	528	560	428	461	229	673	784	664.5	526	353
411	585	592	492	492	285	693	678	787	477	617
412	623	534	863	441	244	638	784	678	532	548
413	391	567	475	462	299	680	796	681.5	547	543
414	504	532	866	446	307	647	583	655	478	385
415	558	513	449	424	530	620	565.5	669.5	543	498
416	503	596	479	496	256	699	791	777	350	330
417	351	584	383	483	320	684	663	745	562	324
418	592	563	480	464	275	649	758	713	530	445
419	514	541	406	448	330	610	678	661	460	520
420	492	540	423	435	311	648	494.5	623	455	307
421	618	555	460	455	209	651	776	687	549	569
422	615	519	388	417	534	655	776	645	424	444
423	293	463	435	370	622	582	747.5	588	494	511
424	462	573	448	469	318	678	784	734	366	523
425	491	562	477	467	309	687	665.5	729	395	590
426	563	487	432	389	588	605	753.5	590	403	606
427	468	538	490	416	618	603	681.5	633.5	521	465
428	559	558	422	468	493	623	673	680	553	526
429	432	586	416	484	308	688	734.5	762	602	621
430	449	537	441	437	201	671	729.5	683.5	512	598
431	430	497	413	410	327	650	659.5	632	540	458
432	281	585	494	477	394	625	762	710	427	456
433	389	566	481	465	328	659	758	719	560	528
434	307	502	860	403	315	640	613	616	457	417
435	454	591	399	489	246	681	791	753	361	551
436	417	565	459	463	301	675	742.5	711	519	527
437	481	533	474	433	257	654	560	644	508	536
438	499	583	873	486	599	622	719	715	546	580
439	569	557	439	457	284	669	659.5	674	398	592
440	392	489	401	388	290	635	650	601.5	379	333

Table S13: The true ranks (tRank) and the ranks predicted by SR (spectral radius), SG (spectral gap), NCo (natural connectivity), ACo (algebraic connectivity), ERe (effective resistance), STC (spanning tree count), HE (heterogeneity), PCR, and iPCR, respectively. [Part 12/30]

id	tRank	SR	SG	NCo	ACo	ERe	STC	HE	PCR	iPCR
441	564	511	430	409	258	662	654.5	642	452	464
442	393	569	375	472	525	661	738.5	719	410	561
443	562	590	486	493	245	677	563.5	744	566	489
444	510	520	385	425	248	670	668.5	630	420	409
445	371	539	420	438	282	630	796	652	482	555
446	643	500	395	412	196	634	665.5	604	386	433
447	515	485	453	381	552	581	738.5	617	459	361
448	415	503	436	401	195	660	769	612	468	374
449	447	506	456	405	281	626	483	609	548	546
450	575	553	472	458	22	697	570	704.5	488	338
451	471	598	447	499	393	698	524	780	518	519
452	319	525	409	429	544	607	644	647	340	304
453	581	570	468	470	566	615	747.5	692.5	505	402
454	412	521	483	422	597	643	668.5	694	573	609
455	438	530	476	415	117	633	742.5	639	569	534
456	477	522	470	413	260	691	734.5	629	481	420
457	672	493	426	393	643	594	753.5	618.5	428	412
458	529	495	461	382	251	616	663	608	557	475
459	556	528	469	426	546	608	732	648	584	488
460	465	577	452	475	292	694	762	736	556	422
461	531	551	396	453	247	668	485	701	357	506
462	353	599	875	498	601	685	722	800	306	531
463	580	579	444	488	241	657	565.5	719	413	303
464	613	536	454	440	295	641	784	650	279	332
465	611	589	487	487	511	674	753.5	757	448	323
466	524	507	386	421	280	624	583	624	503	454
467	493	600	874	500	294	692	617	795	356	486
468	356	597	484	497	521	696	769	796	581	460
469	627	578	443	478	262	646	673	716	443	562
470	530	546	478	444	221	695	794	669.5	475	434
471	467	582	457	479	277	663	784	760	498	567
472	403	457	846	345	522	600	706	581	541	362
473	547	572	495	449	385	614	769	666	527	382
474	593	593	455	491	273	682	784	767	480	594
475	445	574	493	454	298	652	758	675	504	426
476	439	594	489	494	261	700	747.5	786	341	596
477	407	524	424	428	500	628	753.5	656	597	345
478	401	547	869	432	293	656	725.5	651	367	521
479	526	526	381	420	297	621	776	646	456	586
480	552	510	871	399	186	619	705	618.5	484	340

Table S14: The true ranks (tRank) and the ranks predicted by SR (spectral radius), SG (spectral gap), NCo (natural connectivity), ACo (algebraic connectivity), ERe (effective resistance), STC (spanning tree count), HE (heterogeneity), PCR, and iPCR, respectively. [Part 13/30]

id	tRank	SR	SG	NCo	ACo	ERe	STC	HE	PCR	iPCR
481	587	464	466	363	264	653	485	585	535	631
482	507	595	471	495	591	672	647.5	769	586	571
483	603	581	488	480	581	639	791	700	601	587
484	632	505	465	404	322	645	791	641	517	524
485	633	571	446	476	279	689	729.5	759	588	512
486	582	554	458	450	194	667	776	683.5	567	368
487	420	588	491	490	556	665	663	750.5	449	358
488	461	561	451	474	240	690	784	739	552	440
489	541	514	433	411	613	631	765	625	390	350
490	498	548	445	459	259	636	776	690	479	579
491	673	531	485	418	316	637	656.5	633.5	432	554
492	495	550	868	460	265	676	522	691	438	443
493	269	542	421	436	200	658	732	654	590	572
494	626	529	404	442	266	679	668.5	649	391	501
495	543	543	463	434	296	618	784	628	440	366
496	597	535	400	431	524	627	656.5	640	513	334
497	335	559	427	451	271	642	747.5	664.5	429	589
498	284	477	462	374	516	617	769	595	473	542
499	590	552	482	456	451	632	559	669.5	404	576
500	394	518	438	427	310	609	769	635	439	474
501	49	873	721	872	662	293	1086	550	180	98
502	231	844	683	844	754	228	1158	451	261	63
503	279	805	938	804	775	223	1149.5	406.5	243	33
504	381	756	654	733	914	183	1166	388	334	196
505	285	879	694	882	777	262	1161	541	235	50
506	270	827	917	826	762	257	955.5	462	260	228
507	28	810	633	809	800	212	1111.5	418.5	192	252
508	108	881	647	883	680	238	1170.5	518	239	219
509	325	768	685	761	1025	211	924	393	296	92
510	332	848	646	848	269	284	1194	456	162	32
511	337	861	695	861	761	243	1111.5	458	182	62
512	89	823	702	822	795	225	1162.5	413	200	173
513	94	886	675	886	659	287	873.5	562	328	236
514	229	872	944	873	706	273	1152	553	184	212
515	14	878	716	881	650	275	1117	545	290	47
516	153	892	943	890	323	297	961	551	300	124
517	297	825	656	823	744	280	1175.5	453	322	291
518	81	899	946	899	988	282	1200	613	293	3
519	176	792	620	791	757	235	1111.5	406.5	240	171
520	74	849	713	849	933	254	1002	467	252	96

Table S15: The true ranks (tRank) and the ranks predicted by SR (spectral radius), SG (spectral gap), NCo (natural connectivity), ACo (algebraic connectivity), ERe (effective resistance), STC (spanning tree count), HE (heterogeneity), PCR, and iPCR, respectively. [Part 14/30]

id	tRank	SR	SG	NCo	ACo	ERe	STC	HE	PCR	iPCR
521	69	877	941	875	805	247	1152	511	338	42
522	66	891	718	892	924	277	1169	563	269	138
523	442	860	696	855	341	294	1189	472	304	99
524	15	783	686	773	781	216	1121.5	412	321	127
525	240	867	669	865	603	252	996	507	198	246
526	4	790	667	784	991	188	1006.5	390.5	291	188
527	122	842	692	842	948	224	1173	452	273	109
528	303	896	632	897	305	299	1100.5	596	265	150
529	306	866	643	870	735	244	1100.5	473	311	163
530	224	836	698	837	794	231	1090.5	454	190	93
531	123	785	712	781	767	210	1008.5	396.5	232	41
532	11	882	942	880	766	266	1152	520	194	224
533	90	885	705	885	700	267	999	479	220	197
534	33	884	722	878	807	263	1083	505	294	118
535	24	820	651	821	268	286	1117	428	280	29
536	100	799	649	802	286	268	1117	420	316	278
537	186	832	626	831	737	239	1125.5	444	207	107
538	190	894	945	894	945	271	936.5	574	310	21
539	483	856	701	851	959	237	1194	466	317	20
540	223	855	690	862	997	256	1016	496	216	95
541	107	851	597	860	793	251	1086	500	206	110
542	32	789	608	786	1005	175	1095	424	295	149
543	336	767	679	749	533	221	1192	381	222	46
544	246	794	645	792	696	203	1184	399	332	26
545	60	865	655	867	790	255	1095	461	150	169
546	200	864	693	864	746	289	1105	528	147	186
547	232	793	708	796	1027	197	997	401.5	271	90
548	291	838	684	836	789	236	1105	436	336	294
549	106	893	671	893	739	291	1095	570	237	60
550	142	868	616	871	710	246	1090.5	469	169	104
551	117	771	664	754	743	222	1166	390.5	244	115
552	174	839	687	841	755	259	1100.5	494	268	39
553	187	831	641	830	955	213	926	423	258	69
554	149	888	689	888	718	295	1179	543.5	264	101
555	290	818	630	814	596	234	1197.5	404	302	265
556	257	862	676	853	778	278	1095	480	247	106
557	211	897	677	896	302	296	1189	587	323	161
558	111	854	697	854	779	248	1179	517	346	253
559	76	887	662	887	941	264	1058	559	284	77
560	282	874	642	876	962	240	1166	519	315	239

Table S16: The true ranks (tRank) and the ranks predicted by SR (spectral radius), SG (spectral gap), NCo (natural connectivity), ACo (algebraic connectivity), ERe (effective resistance), STC (spanning tree count), HE (heterogeneity), PCR, and iPCR, respectively. [Part 15/30]

id	tRank	SR	SG	NCo	ACo	ERe	STC	HE	PCR	iPCR
561	18	890	668	889	725	269	1121.5	523	249	15
562	102	852	711	858	750	261	1189	483.5	217	145
563	125	863	644	863	587	274	1129	558	369	143
564	133	869	707	866	771	283	1173	525	219	275
565	12	900	720	900	335	300	918	636	250	170
566	329	729	898	686	695	134	1156	352	256	37
567	252	875	715	874	336	298	1166	565	173	31
568	334	806	631	811	325	249	1154.5	431	208	132
569	87	828	681	832	773	276	1081	463	117	27
570	5	846	717	846	733	270	1189	536	259	152
571	328	829	672	827	788	229	1081	439	292	147
572	48	859	670	856	688	288	1100.5	483.5	342	36
573	195	840	714	839	936	226	1189	471	152	146
574	185	770	918	764	321	227	1045.5	392	324	256
575	128	837	703	835	765	245	1184	459	148	215
576	103	889	614	891	769	290	936.5	508	282	76
577	144	898	625	898	339	292	924	583	253	67
578	191	746	622	719	832	196	921.5	377	275	82
579	277	841	688	843	681	241	1090.5	446	246	25
580	167	808	700	806	966	206	1179	432	166	75
581	245	871	657	869	986	260	1100.5	521	272	58
582	85	834	691	833	742	232	1086	460	351	64
583	7	858	940	857	791	272	1132	513.5	204	176
584	220	791	706	789	736	218	1173	418.5	262	120
585	162	883	710	884	776	250	1090.5	529	225	24
586	116	801	650	801	678	207	1019.5	414	274	38
587	75	726	665	678	751	173	1006.5	345	226	159
588	45	857	723	859	747	258	1170.5	504	277	198
589	248	809	659	813	728	242	1125.5	434	178	136
590	50	826	709	828	999	220	1111.5	440	288	73
591	375	833	699	834	956	233	1179	450	241	108
592	228	895	724	895	687	285	1179	578	285	140
593	112	812	673	808	942	230	1004.5	425	205	270
594	486	803	623	803	965	195	1038.5	415	144	295
595	254	845	719	847	764	281	1100.5	503	325	243
596	63	774	660	765	721	214	1175.5	395	197	223
597	119	787	624	785	784	198	1032	377	176	65
598	441	880	652	877	698	279	1002	560	313	9
599	212	847	678	845	715	265	1184	457	255	254
600	262	870	658	868	701	253	1086	486	234	269

Table S17: The true ranks (tRank) and the ranks predicted by SR (spectral radius), SG (spectral gap), NCo (natural connectivity), ACo (algebraic connectivity), ERe (effective resistance), STC (spanning tree count), HE (heterogeneity), PCR, and iPCR, respectively. [Part 16/30]

id	tRank	SR	SG	NCo	ACo	ERe	STC	HE	PCR	iPCR
601	1005	139	801	41	59	832	315.5	727	677	759
602	817	124	785	19	355	844	164.5	728	753	872
603	750	154	800	46	338	820	122.5	688.5	933	858
604	987	160	116	69	276	848	127.5	770	620	912
605	828	193	804	83	206	893	144	788	660	847
606	820	162	175	58	361	829	127.5	706	610	900
607	812	196	167	92	300	887	74.5	771	943	855
608	658	134	803	49	43	824	130.5	703	850	881
609	778	112	111	6	263	830	30	637.5	617	879
610	970	178	794	75	313	890	305	774	665	834
611	766	192	211	101	354	888	48	798	633	740
612	802	194	170	91	96	897	269	783.5	663	933
613	874	163	168	42	197	889	305	761	656	984
614	826	120	779	10	306	851	100	659	774	889
615	604	128	173	36	359	827	106.5	659	813	770
616	969	170	187	71	352	860	213	772.5	918	875
617	885	118	782	9	332	819	199	663	694	841
618	995	149	784	17	267	831	308.5	730.5	712	904
619	763	137	783	16	351	841	288.5	692.5	791	885
620	745	129	775	44	164	858	91.5	685.5	664	914
621	944	207	108	74	356	846	275	763.5	737	785
622	1006	183	124	98	331	894	312	799	912	816
623	781	123	789	50	224	872	21	740.5	683	842
624	700	156	121	105	233	898	2	781.5	932	862
625	835	159	793	40	287	876	186	696	746	776
626	886	148	791	53	235	855	89	712	705	795
627	780	151	193	72	220	865	4	685.5	969	804
628	831	166	141	73	288	842	94	738	624	919
629	907	173	127	67	358	866	400	766	704	780
630	771	133	125	15	230	869	287	696	673	857
631	919	117	181	54	377	853	47	696	821	849
632	922	175	123	87	253	868	305	776	655	753
633	761	158	805	95	231	871	1	743	650	808
634	917	121	777	25	239	822	35.5	669.5	652	773
635	1022	127	130	29	47	833	226.5	699	690	772
636	847	132	115	14	369	828	302.5	709	644	725
637	908	152	120	62	353	834	108.5	735	751	819
638	759	172	802	76	376	852	272.5	746.5	619	910
639	999	164	103	45	347	879	296.5	707	848	764
640	865	176	226	66	158	895	331.5	772.5	675	908

Table S18: The true ranks (tRank) and the ranks predicted by SR (spectral radius), SG (spectral gap), NCo (natural connectivity), ACo (algebraic connectivity), ERe (effective resistance), STC (spanning tree count), HE (heterogeneity), PCR, and iPCR, respectively. [Part 17/30]

id	tRank	SR	SG	NCo	ACo	ERe	STC	HE	PCR	iPCR
641	979	169	795	60	184	882	70.5	746.5	967	871
642	683	190	182	85	362	864	31.5	749	649	959
643	710	142	105	26	123	814	321	688.5	647	948
644	723	107	772	8	274	812	63	605	707	754
645	881	182	161	88	6	900	7	791	868	832
646	816	113	787	33	374	809	15	626.5	638	757
647	790	104	771	1	236	805	85.5	575	757	768
648	993	155	101	57	363	810	12.5	643	797	801
649	841	102	150	4	125	803	242	615	608	960
650	940	145	138	68	346	870	265.5	717	910	779
651	725	147	799	24	312	811	186	679	765	863
652	767	198	814	89	38	899	186	797	679	866
653	655	188	812	80	89	892	298	794	722	884
654	814	202	143	79	372	836	380.5	778	905	829
655	803	168	114	61	317	843	186	732	696	843
656	764	136	778	31	4	880	279	748	695	895
657	774	197	183	106	367	863	116.5	793	684	815
658	716	126	136	13	203	840	373	672	606	949
659	876	161	194	43	46	885	127.5	708	756	883
660	861	185	816	93	337	875	12.5	755	689	856
661	617	122	142	23	348	854	178.5	724	702	788
662	992	179	104	65	350	884	133.5	758	629	731
663	734	131	781	30	368	817	133.5	698	627	793
664	864	177	808	59	242	881	265.5	785	856	800
665	788	105	134	27	222	806	186	622	777	860
666	823	165	809	81	228	878	96	789.5	630	898
667	718	171	798	78	340	883	130.5	768	714	935
668	758	167	797	51	118	891	272.5	756	792	840
669	521	186	118	70	304	896	373	779	623	870
670	869	212	106	94	329	849	186	792	909	714
671	637	150	788	21	364	850	284	754	855	852
672	837	189	811	86	238	886	261.5	775	838	838
673	978	101	774	3	384	801	293	600	631	790
674	836	135	119	28	326	862	386	721	670	851
675	785	184	815	90	375	877	85.5	781.5	1004	830
676	1012	153	796	32	344	847	186	740.5	668	813
677	721	130	192	37	291	838	139	676.5	762	836
678	691	125	110	35	333	804	112	676.5	936	749
679	696	110	773	7	289	818	139	610	834	947
680	880	138	126	47	343	835	133.5	702	744	828

Table S19: The true ranks (tRank) and the ranks predicted by SR (spectral radius), SG (spectral gap), NCo (natural connectivity), ACo (algebraic connectivity), ERe (effective resistance), STC (spanning tree count), HE (heterogeneity), PCR, and iPCR, respectively. [Part 18/30]

id	tRank	SR	SG	NCo	ACo	ERe	STC	HE	PCR	iPCR
681	933	114	184	20	365	821	229.5	659	622	890
682	742	106	133	11	357	802	19.5	598.5	676	722
683	825	103	117	2	366	807	302.5	621	716	886
684	958	119	113	52	250	815	22	637.5	820	848
685	733	109	780	18	371	808	10	657	922	844
686	854	144	790	38	373	823	151	724	661	945
687	801	146	178	39	30	825	364.5	724	708	907
688	706	157	146	63	314	861	70.5	726	685	891
689	811	108	786	5	319	826	171	626.5	750	954
690	935	141	137	34	349	839	220.5	722	680	906
691	808	116	806	22	360	813	277	653	809	846
692	822	181	128	82	223	859	156.5	742	635	775
693	1015	174	155	77	345	845	257.5	765	639	925
694	770	143	792	56	270	857	67	730.5	724	756
695	888	180	807	64	342	867	144	763.5	632	880
696	863	191	810	96	278	874	51	783.5	779	811
697	968	111	776	48	62	837	11	673	946	825
698	871	140	160	55	370	856	216.5	752	720	817
699	899	201	819	84	193	873	312	789.5	736	782
700	858	115	109	12	303	816	102	631	678	867
701	609	427	414	329	646	542	673	515.5	349	508
702	513	407	827	307	381	539	496.5	445	434	327
703	354	436	362	339	642	517	501	492.5	287	406
704	560	401	822	302	717	483	713.5	448	212	448
705	359	491	434	396	420	587	515.5	576	554	375
706	595	437	836	336	799	523	711.5	490.5	335	430
707	573	454	417	368	543	560	436	537	242	349
708	578	428	389	330	568	534	466.5	497	309	505
709	544	429	419	337	611	563	437	481.5	174	624
710	425	481	848	379	768	551	613	554	388	427
711	469	498	363	398	738	566	488.5	592	450	487
712	352	412	828	313	550	529	473.5	470	523	389
713	484	483	864	392	535	583	432	566.5	314	428
714	517	433	840	327	548	549	456	501	406	564
715	426	467	398	362	512	586	570	561	492	351
716	614	461	393	356	520	509	776	526	133	386
717	642	504	379	400	505	589	632.5	577	251	315
718	568	418	834	322	503	547	620.5	464	209	552
719	343	411	366	318	606	506	599.5	455	501	595
720	522	438	352	357	570	518	508	515.5	267	462

Table S20: The true ranks (tRank) and the ranks predicted by SR (spectral radius), SG (spectral gap), NCo (natural connectivity), ACo (algebraic connectivity), ERe (effective resistance), STC (spanning tree count), HE (heterogeneity), PCR, and iPCR, respectively. [Part 19/30]

id	tRank	SR	SG	NCo	ACo	ERe	STC	HE	PCR	iPCR
721	384	471	854	351	576	559	587	547	397	377
722	362	453	858	347	638	525	439	513.5	392	317
723	505	450	842	344	529	585	457	542	371	550
724	535	473	415	386	609	578	471.5	564	359	337
725	594	512	392	414	647	604	587	611	400	421
726	366	480	851	377	554	602	620.5	566.5	353	473
727	457	488	394	397	689	572	444	549	318	522
728	576	462	387	366	579	596	673	569	289	610
729	416	419	826	316	447	565	595.5	485	329	485
730	258	405	829	303	619	470	715.5	422	447	482
731	571	470	857	360	536	553	508	546	298	481
732	370	425	830	314	382	544	724	481.5	139	626
733	423	458	856	364	674	545	449	543.5	571	447
734	300	445	360	349	780	530	626	522	355	425
735	537	460	850	372	334	595	424	556.5	596	593
736	534	494	412	395	389	552	678	571	245	525
737	479	515	408	419	510	612	595.5	606.5	305	497
738	238	431	831	348	538	540	501	487.5	266	510
739	525	544	872	445	782	564	572	586	437	437
740	509	432	391	333	387	574	577	490.5	497	515
741	314	499	403	394	577	568	618	581	476	492
742	350	465	849	359	564	536	487	530.5	352	346
743	405	408	351	310	518	468	573.5	443	327	438
744	550	509	418	402	758	571	654.5	594	387	565
745	539	406	821	305	479	464	711.5	416	436	429
746	602	442	832	341	390	556	494.5	498	344	367
747	473	421	371	325	562	521	636	506	358	490
748	435	420	405	317	506	512	562	487.5	254	483
749	286	449	370	353	808	533	491.5	540	299	472
750	444	424	369	323	392	561	650	499	575	577
751	459	455	353	350	802	497	496.5	512	375	328
752	360	508	364	408	553	584	799.5	584	394	411
753	588	468	402	384	497	575	466.5	533	376	372
754	330	456	839	354	685	537	518.5	555	339	378
755	599	459	372	358	574	526	678	534.5	233	604
756	382	474	367	376	573	606	537	573	537	319
757	378	448	354	365	582	558	477.5	534.5	307	312
758	536	435	852	335	595	554	451.5	475	561	314
759	702	545	865	443	555	588	692	606.5	238	591
760	451	575	361	471	531	611	607.5	667	354	453

Table S21: The true ranks (tRank) and the ranks predicted by SR (spectral radius), SG (spectral gap), NCo (natural connectivity), ACo (algebraic connectivity), ERe (effective resistance), STC (spanning tree count), HE (heterogeneity), PCR, and iPCR, respectively. [Part 20/30]

id	tRank	SR	SG	NCo	ACo	ERe	STC	HE	PCR	iPCR
761	638	410	365	311	677	477	532	426	453	507
762	549	492	429	391	645	567	776	591	303	549
763	349	443	847	355	594	569	461	556.5	446	539
764	204	447	357	352	630	541	434	502	472	496
765	460	549	870	447	575	577	425	601.5	365	359
766	565	416	355	331	378	502	537	476	372	316
767	456	490	861	387	380	593	471.5	589	331	394
768	317	469	407	361	495	598	567	552	466	563
769	373	439	835	324	631	527	638.5	527	419	321
770	540	422	384	326	547	507	736	495	308	495
771	475	486	410	380	514	579	575.5	568	383	318
772	546	415	358	320	605	437	430	437	345	336
773	408	476	359	373	607	555	624	538.5	389	343
774	388	501	380	407	664	580	610	614	297	581
775	341	414	844	312	620	535	593.5	465	462	397
776	344	452	853	338	803	516	610	509	563	390
777	390	516	855	430	602	599	411	597	431	360
778	385	482	862	385	396	562	454.5	530.5	408	379
779	511	426	356	332	663	514	709.5	510	231	484
780	482	423	837	319	406	573	479	474	551	502
781	478	440	368	342	745	466	580	478	463	471
782	400	402	397	301	541	461	796	411	343	418
783	387	451	437	334	586	543	762	468	377	392
784	497	472	838	375	615	591	690	579	458	369
785	472	441	841	346	563	524	620.5	492.5	319	532
786	538	417	411	315	589	472	641	447	283	347
787	620	479	843	383	561	576	715.5	581	347	441
788	315	430	374	340	567	538	615.5	489	411	371
789	213	444	382	328	580	546	703	477	568	557
790	512	403	824	304	559	441	525.5	408	539	446
791	239	413	823	309	801	462	587	441.5	469	352
792	302	475	859	371	498	548	464	538.5	528	467
793	386	517	867	406	584	592	518.5	603	257	415
794	488	478	373	369	731	557	547.5	548	380	396
795	236	434	377	321	386	532	699.5	532	416	322
796	331	446	845	343	419	550	723	524	430	407
797	654	404	825	306	657	445	798	417	301	504
798	496	409	833	308	592	492	590	441.5	326	395
799	520	523	390	423	413	590	624	620	402	354
800	255	466	425	367	655	570	632.5	572	385	410

Table S22: The true ranks (tRank) and the ranks predicted by SR (spectral radius), SG (spectral gap), NCo (natural connectivity), ACo (algebraic connectivity), ERe (effective resistance), STC (spanning tree count), HE (heterogeneity), PCR, and iPCR, respectively. [Part 21/30]

id	tRank	SR	SG	NCo	ACo	ERe	STC	HE	PCR	iPCR
801	222	761	604	750	1080	147	1166	361	39	263
802	86	717	901	657	716	151	827	331	168	274
803	261	714	884	643	624	121	830.5	311.5	91	226
804	130	730	893	691	1002	140	863	330	236	122
805	256	821	921	817	824	219	1068.5	410	64	151
806	347	807	924	812	792	180	852	403	202	259
807	326	735	634	716	943	185	836.5	341	116	257
808	109	702	876	604	947	101	931	302	163	142
809	37	759	925	744	927	177	1032	364	164	116
810	199	712	601	636	934	97	936.5	320	7	205
811	67	876	628	879	811	202	895	449	143	229
812	288	786	599	790	983	181	868.5	382	270	174
813	83	747	894	713	923	113	1068.5	333	177	216
814	305	732	899	690	797	167	942.5	339	110	234
815	71	754	619	738	1018	124	968	338	214	283
816	70	816	629	819	970	194	955.5	405	42	250
817	182	772	935	760	939	141	1024.5	366	103	79
818	177	731	637	695	774	129	872	322	4	258
819	166	743	897	711	722	125	988	334	167	121
820	93	715	916	640	1023	104	985.5	317	11	284
821	118	724	883	664	670	136	1058	323	159	185
822	215	748	661	721	973	135	1035	337	70	287
823	201	738	890	704	989	154	856	350	227	134
824	25	835	653	838	796	191	820	421	276	272
825	158	716	615	661	726	145	845	321	154	242
826	168	788	913	779	1003	170	1045.5	368.5	23	83
827	34	736	910	706	1100	126	982	327.5	53	49
828	184	753	888	729	798	182	840	326	121	125
829	17	704	879	610	1096	85	976.5	304	132	172
830	365	721	900	663	682	153	1148	324	170	141
831	135	758	612	746	1037	152	1032	348	15	245
832	22	722	912	660	708	116	901.5	308	127	166
833	214	796	930	795	671	204	1078	371	86	100
834	192	778	934	767	937	178	1138.5	370	44	210
835	197	710	878	626	1042	102	1160	310	125	162
836	95	853	936	852	1066	190	813.5	435	215	139
837	47	779	929	769	930	122	985.5	362	38	247
838	35	811	926	807	978	176	929.5	398	120	51
839	105	815	704	818	809	201	871	400	6	297
840	209	804	903	805	815	193	1132	394	107	255

Table S23: The true ranks (tRank) and the ranks predicted by SR (spectral radius), SG (spectral gap), NCo (natural connectivity), ACo (algebraic connectivity), ERe (effective resistance), STC (spanning tree count), HE (heterogeneity), PCR, and iPCR, respectively. [Part 22/30]

id	tRank	SR	SG	NCo	ACo	ERe	STC	HE	PCR	iPCR
841	237	797	931	798	703	217	1047.5	385	93	277
842	260	713	607	631	1200	74	1086	303	17	232
843	26	781	933	782	931	158	821	383	105	168
844	299	739	613	720	763	139	863	358	145	279
845	172	814	927	815	975	164	1066	396.5	32	119
846	217	707	892	622	957	115	885.5	316	183	293
847	226	773	895	763	944	160	888	342	185	129
848	145	766	635	755	691	156	920	365	20	261
849	251	764	663	747	917	128	999	332	40	112
850	77	780	666	772	759	179	1107.5	375	9	241
851	395	775	939	770	994	155	973	380	281	300
852	283	719	617	675	1087	144	968	336	175	102
853	205	741	682	709	1034	118	1162.5	335	1	208
854	140	777	902	766	967	142	933.5	360	248	180
855	171	727	906	683	976	133	833	325	221	220
856	91	723	627	672	614	159	1028.5	315	75	266
857	154	750	611	731	995	171	898.5	354	160	213
858	157	751	908	728	853	165	980	373	134	218
859	31	765	598	759	693	187	882	356.5	129	288
860	227	703	880	609	992	107	1049.5	307	165	148
861	43	737	609	710	920	127	877.5	343	92	105
862	198	830	621	829	786	200	958.5	427	49	123
863	137	800	923	793	702	189	1129	386	71	281
864	241	819	638	820	932	208	866	401.5	52	221
865	179	755	639	739	1014	148	999	384	31	97
866	56	763	610	756	960	149	875	353	101	231
867	55	725	886	674	770	117	1071.5	329	68	187
868	101	784	909	776	921	186	991	356.5	28	194
869	173	795	648	799	1089	161	904	377	45	289
870	36	752	887	722	528	172	1117	355	66	167
871	188	824	937	824	980	205	1047.5	433	286	177
872	141	709	881	618	1033	96	1053.5	306	51	227
873	127	711	605	630	979	108	857	314	124	154
874	235	742	915	715	683	184	1149.5	340	161	71
875	443	757	596	743	1044	131	812	347	119	282
876	242	798	920	794	1028	137	946	379	59	117
877	54	782	919	775	1149	150	1053.5	387	187	233
878	98	749	602	727	1004	132	951.5	351	60	57
879	96	745	928	708	1019	123	985.5	327.5	94	290
880	380	850	600	850	961	209	927	438	128	203

Table S24: The true ranks (tRank) and the ranks predicted by SR (spectral radius), SG (spectral gap), NCo (natural connectivity), ACo (algebraic connectivity), ERe (effective resistance), STC (spanning tree count), HE (heterogeneity), PCR, and iPCR, respectively. [Part 23/30]

id	tRank	SR	SG	NCo	ACo	ERe	STC	HE	PCR	iPCR
881	189	776	603	771	964	138	1058	368.5	95	230
882	159	744	905	723	783	143	853	349	131	175
883	65	802	922	800	969	162	893	372	196	244
884	156	718	606	653	963	103	1147	313	87	103
885	292	769	680	751	720	168	924	374	112	217
886	99	740	904	712	679	166	896	344	141	114
887	131	762	914	748	972	146	961	359	18	206
888	136	706	885	624	812	112	810	305	130	235
889	57	822	636	825	968	215	1011.5	430	89	262
890	62	760	907	742	977	163	968	367	108	209
891	327	817	640	816	940	199	1079	409	2	298
892	196	843	674	840	996	174	1111.5	429	25	193
893	298	705	896	614	756	130	1044	311.5	22	178
894	59	708	882	617	953	119	1028.5	309	263	192
895	253	728	911	682	1009	109	1021	346	218	286
896	38	701	877	601	753	99	1004.5	301	189	128
897	126	720	618	668	952	120	836.5	318	140	199
898	155	733	889	693	667	157	911.5	319	109	181
899	259	734	891	698	900	169	813.5	363	104	144
900	234	813	932	810	929	192	1062	389	72	135
901	703	3	32	202	234	902	82	2	799	666
902	707	5	41	206	114	940	389.5	5	923	660
903	807	83	75	285	23	1025	40	91	835	649
904	553	4	9	214	110	917	191.5	3	796	796
905	744	43	90	225	75	967	162	88.5	782	703
906	579	88	26	282	52	980	203	127	831	746
907	741	12	88	227	174	911	249	13	703	647
908	715	25	61	224	207	935	194.5	87	810	679
909	682	86	85	272	40	1015	159.5	111	729	619
910	799	65	53	236	95	951	312	92.5	739	723
911	551	100	35	292	70	1045	249	246	776	669
912	635	8	7	217	109	909	261.5	8.5	812	612
913	860	45	62	231	198	950	164.5	95.5	939	716
914	932	37	58	205	104	949	300	55	961	628
915	794	49	36	260	78	923	63	24.5	826	671
916	644	75	64	255	49	963	386	95.5	921	712
917	832	89	87	262	112	1002	325	145	851	850
918	772	39	3	291	32	968	236	46.5	817	958
919	904	35	46	283	73	982	24	50	876	709
920	674	66	84	281	63	1026	49	71.5	911	750

Table S25: The true ranks (tRank) and the ranks predicted by SR (spectral radius), SG (spectral gap), NCo (natural connectivity), ACo (algebraic connectivity), ERe (effective resistance), STC (spanning tree count), HE (heterogeneity), PCR, and iPCR, respectively. [Part 24/30]

id	tRank	SR	SG	NCo	ACo	ERe	STC	HE	PCR	iPCR
921	704	76	98	264	99	992	307	64	763	691
922	727	56	51	263	31	981	29	80	768	688
923	698	29	37	253	26	1008	55	43	743	697
924	577	78	69	270	150	960	44	39	688	784
925	878	41	25	259	227	927	168.5	52.5	926	710
926	678	68	80	300	121	1013	97.5	148	735	670
927	714	71	17	269	205	962	59	44	930	745
928	591	96	100	299	83	1052	14	198	859	689
929	797	53	65	284	129	978	290	81	833	903
930	680	55	45	228	149	928	164.5	39	898	641
931	586	63	96	235	212	948	159.5	92.5	772	687
932	693	16	68	207	107	944	364.5	31.5	731	627
933	671	57	86	242	28	1018	178.5	48	802	792
934	555	64	49	271	165	964	97.5	56.5	869	603
935	668	69	55	295	98	1024	17	18.5	906	711
936	736	97	70	254	97	1010	265.5	148	896	662
937	619	73	12	273	191	976	220.5	128	857	803
938	795	79	44	267	177	979	139	83	745	633
939	909	47	60	248	60	995	194.5	71.5	846	651
940	641	60	77	258	141	985	44	78	804	602
941	652	42	89	216	2	997	272.5	69	852	659
942	598	28	23	274	53	947	63	76	786	733
943	684	33	54	221	124	937	277	26	789	648
944	687	77	43	293	182	988	85.5	100	798	755
945	748	31	74	218	77	971	27	27.5	878	864
946	566	59	42	240	103	934	51	52.5	749	704
947	660	6	21	265	163	925	99	10.5	790	806
948	862	50	22	223	204	933	224	22.5	748	706
949	676	26	11	245	67	958	347	24.5	837	677
950	953	92	66	287	135	1029	28	184	861	766
951	694	20	13	232	122	924	300	13	865	769
952	548	13	40	210	180	919	94	6	764	620
953	612	62	52	288	126	966	319	90	726	705
954	600	82	78	290	106	1014	178.5	141.5	842	930
955	610	10	19	275	211	930	5	20	803	690
956	711	72	33	294	137	1011	85.5	125	775	774
957	677	58	14	252	199	926	114.5	88.5	752	732
958	856	81	4	277	160	965	94	117	945	644
959	739	17	8	212	108	916	139	8.5	771	728
960	879	80	63	261	166	959	125	52.5	881	658

Table S26: The true ranks (tRank) and the ranks predicted by SR (spectral radius), SG (spectral gap), NCo (natural connectivity), ACo (algebraic connectivity), ERe (effective resistance), STC (spanning tree count), HE (heterogeneity), PCR, and iPCR, respectively. [Part 25/30]

id	tRank	SR	SG	NCo	ACo	ERe	STC	HE	PCR	iPCR
961	663	36	99	209	151	973	151	65.5	830	682
962	728	90	2	250	29	987	293	130.5	742	634
963	630	27	72	208	105	956	394	67	875	799
964	833	98	81	278	146	1012	156.5	205	960	853
965	730	9	39	213	181	906	89	10.5	761	650
966	670	94	6	298	215	972	83	56.5	823	818
967	855	95	83	280	142	1006	281	154	741	635
968	648	74	79	233	16	1003	351	161	815	736
969	650	30	5	226	145	954	106.5	30	892	676
970	821	23	28	229	217	913	18	33	740	738
971	769	18	48	203	130	915	397	7	657	787
972	787	46	95	211	179	955	325	46.5	972	943
973	892	24	1	234	131	908	173.5	29	671	700
974	567	99	97	297	65	1042	209.5	214	733	667
975	622	91	94	279	213	989	77	141.5	829	672
976	717	11	31	246	218	920	173.5	22.5	862	831
977	768	22	50	243	79	961	168.5	21	937	744
978	845	38	34	241	156	977	89	58.5	767	652
979	784	67	16	289	34	994	116.5	148	770	719
980	667	1	18	201	254	904	285	1	787	789
981	557	54	91	238	72	957	55	65.5	785	721
982	606	34	38	256	189	969	51	52.5	958	640
983	636	52	57	247	37	1016	236	39	755	814
984	732	61	82	239	133	953	110.5	34	836	630
985	624	48	59	251	84	974	186	122	723	783
986	690	15	10	237	91	952	236	27.5	766	730
987	664	19	15	220	159	929	78	4	914	638
988	724	44	24	276	41	975	31.5	123	873	654
989	634	93	76	266	90	1022	293	151.5	814	786
990	810	87	27	230	88	1021	101	106	794	758
991	926	14	47	204	100	912	206.5	16.5	800	681
992	665	32	30	244	140	945	154	36	935	615
993	607	2	20	257	252	914	3	16.5	769	717
994	608	40	71	249	132	946	194.5	45	734	708
995	818	70	29	268	55	1004	319	130.5	872	614
996	645	85	93	286	74	1036	331.5	151.5	897	642
997	681	21	92	219	64	936	55	18.5	732	737
998	775	84	67	296	138	1009	178.5	102	801	701
999	695	51	56	222	225	941	293	31.5	832	632
1000	605	7	73	215	120	932	6	13	691	809

Table S27: The true ranks (tRank) and the ranks predicted by SR (spectral radius), SG (spectral gap), NCo (natural connectivity), ACo (algebraic connectivity), ERe (effective resistance), STC (spanning tree count), HE (heterogeneity), PCR, and iPCR, respectively. [Part 26/30]

id	tRank	SR	SG	NCo	ACo	ERe	STC	HE	PCR	iPCR
1001	320	304	301	508	654	406	446	79	572	570
1002	455	342	344	564	690	487	406	230	577	568
1003	340	319	294	533	741	416	409.5	170	591	578
1004	266	371	267	585	709	471	549.5	273	531	556
1005	280	308	270	511	632	413	525.5	108	451	494
1006	410	306	251	507	675	402	689	174	538	357
1007	427	327	262	537	621	421	602	155	550	530
1008	368	343	318	539	724	467	409.5	221	514	405
1009	361	381	303	584	616	488	520	249.5	405	222
1010	376	378	330	592	515	484	704	275.5	542	566
1011	275	359	292	566	625	425	441	200	415	363
1012	527	353	259	527	666	456	799.5	239	520	384
1013	396	313	269	510	785	410	523	114	487	413
1014	487	372	295	580	730	493	458	264	545	344
1015	490	356	320	571	585	474	401	262	381	391
1016	321	347	332	544	723	438	590	242	362	439
1017	518	354	334	542	651	449	498.5	258	382	500
1018	322	346	275	557	704	435	637	263	422	311
1019	301	336	265	529	565	424	606	158	491	476
1020	345	379	342	551	608	500	742.5	281	421	493
1021	421	363	260	567	711	455	747.5	267	426	387
1022	311	345	287	572	676	505	427	265.5	401	320
1023	419	369	345	558	668	459	599.5	256.5	600	600
1024	431	316	257	525	542	414	515.5	209	578	373
1025	324	348	339	552	545	476	488.5	237	555	442
1026	474	324	305	512	526	418	542.5	183	407	308
1027	649	333	302	547	649	434	530	222.5	582	424
1028	572	355	282	532	672	490	687	249.5	515	599
1029	363	303	312	509	673	417	480.5	173	364	326
1030	413	314	323	524	684	431	418	185	423	461
1031	489	325	273	522	748	419	545.5	218	589	585
1032	355	331	283	526	772	412	644	197	565	457
1033	369	396	349	587	572	503	707.5	296	378	516
1034	440	397	327	589	714	495	628.5	280	502	583
1035	295	375	350	576	749	498	407.5	277	576	414
1036	508	367	308	528	627	460	563.5	235	489	449
1037	278	400	304	600	539	511	491.5	300	433	388
1038	589	312	253	536	656	422	426	134	337	416
1039	414	366	317	577	571	465	725.5	295	374	305
1040	480	349	296	548	787	432	720.5	210	493	463

Table S28: The true ranks (tRank) and the ranks predicted by SR (spectral radius), SG (spectral gap), NCo (natural connectivity), ACo (algebraic connectivity), ERe (effective resistance), STC (spanning tree count), HE (heterogeneity), PCR, and iPCR, respectively. [Part 27/30]

id	tRank	SR	SG	NCo	ACo	ERe	STC	HE	PCR	iPCR
1041	437	315	321	505	598	404	697	124	312	541
1042	402	374	348	538	617	489	738.5	247	483	364
1043	397	365	299	534	697	463	707.5	243	373	547
1044	418	302	266	503	699	411	709.5	118.5	580	376
1045	339	328	297	565	658	457	404	206	506	540
1046	333	307	276	502	729	405	717.5	85	495	559
1047	216	318	311	518	519	478	578	225.5	536	537
1048	434	394	268	599	513	520	453	278	529	477
1049	312	388	346	562	634	452	769	291	533	514
1050	523	382	326	563	752	443	554.5	269	348	313
1051	501	301	314	501	560	409	610	60	525	419
1052	448	323	285	521	569	427	624	222.5	412	575
1053	377	317	328	517	712	433	530	201	486	529
1054	308	386	340	578	692	501	527.5	286.5	511	560
1055	289	390	331	594	641	494	504.5	286.5	360	479
1056	249	380	337	561	648	510	632.5	282	333	436
1057	357	387	341	575	639	504	459	292.5	509	480
1058	97	344	309	543	661	450	511	220	368	325
1059	446	305	274	506	760	401	580	118.5	363	478
1060	506	339	324	555	727	430	603.5	233	330	301
1061	561	350	281	550	637	469	568	241	471	470
1062	265	389	264	593	705	486	460	289.5	564	616
1063	516	395	307	598	527	519	684.5	289.5	454	342
1064	428	377	284	583	551	442	551	225.5	485	398
1065	398	326	256	556	540	444	627	204	499	370
1066	452	383	306	596	636	515	683	292.5	496	435
1067	383	351	325	546	629	447	537	232	470	503
1068	374	311	252	519	610	415	544	181	490	341
1069	502	370	335	574	740	499	607.5	284	559	466
1070	309	357	279	568	660	453	561	270	464	309
1071	346	384	300	581	732	482	466.5	288	500	339
1072	250	341	278	545	508	496	447.5	260	507	533
1073	409	337	277	549	557	439	421	217	467	348
1074	247	362	333	560	734	475	480.5	245	461	423
1075	450	368	298	597	713	528	414	275.5	435	491
1076	294	361	280	554	604	451	646	248	574	499
1077	406	360	261	570	600	446	583	188	534	553
1078	476	373	286	573	549	473	501	256.5	604	365
1079	379	352	310	569	707	454	405	219	611	605
1080	436	358	329	553	578	485	659.5	251	585	558

Table S29: The true ranks (tRank) and the ranks predicted by SR (spectral radius), SG (spectral gap), NCo (natural connectivity), ACo (algebraic connectivity), ERe (effective resistance), STC (spanning tree count), HE (heterogeneity), PCR, and iPCR, respectively. [Part 28/30]

id	tRank	SR	SG	NCo	ACo	ERe	STC	HE	PCR	iPCR
1081	358	322	313	513	686	426	419	159	474	538
1082	399	334	272	535	626	448	573.5	228	417	535
1083	453	399	263	591	669	480	650	294	393	331
1084	485	391	258	595	694	508	438	299	445	393
1085	424	376	293	582	537	522	504.5	297	320	380
1086	463	321	316	516	583	407	620.5	163	465	329
1087	287	398	322	588	532	513	694	298	524	518
1088	348	340	288	523	523	440	530	195	570	574
1089	458	320	255	514	640	403	732	129	444	431
1090	494	335	271	540	644	458	490	213	370	381
1091	470	364	289	559	623	479	537	254	409	509
1092	542	310	254	515	590	420	451.5	98	425	459
1093	318	393	315	579	507	531	537	265.5	522	588
1094	364	309	338	504	628	408	580	116	594	450
1095	464	338	319	541	804	428	440	227	595	517
1096	243	332	291	531	719	423	605	207	396	401
1097	372	385	336	590	665	481	511	283	399	573
1098	367	329	343	530	612	429	542.5	212	605	513
1099	532	330	290	520	558	436	753.5	176	593	400
1100	596	392	347	586	652	491	477.5	279	558	399
1101	41	697	583	780	982	100	1011.5	272	82	240
1102	104	655	586	676	1088	46	914	179.5	21	78
1103	44	625	521	637	1040	10	1011.5	75	210	14
1104	1	698	503	783	1026	82	1032	238	181	237
1105	219	699	581	787	1065	98	928	274	138	182
1106	180	624	505	649	1068	8	915.5	73.5	223	276
1107	6	696	516	797	1035	114	824	285	36	130
1108	276	675	547	726	998	84	958.5	216	171	299
1109	152	637	576	650	1061	38	807	120	151	200
1110	23	614	592	616	1056	56	866	109.5	115	184
1111	58	644	536	662	1006	54	877.5	136.5	102	45
1112	233	680	512	724	925	86	1132	231	191	6
1113	244	622	548	635	1031	28	991	112.5	80	201
1114	124	662	497	689	1043	42	1016	179.5	16	10
1115	13	607	504	613	1067	23	827	99	137	190
1116	79	664	544	707	1086	32	933.5	175	203	1
1117	19	645	538	669	926	68	946	166	230	204
1118	88	632	556	644	1084	19	946	104	58	88
1119	9	609	524	612	919	20	815	84	78	285
1120	27	684	594	740	935	83	876	208	96	137

Table S30: The true ranks (tRank) and the ranks predicted by SR (spectral radius), SG (spectral gap), NCo (natural connectivity), ACo (algebraic connectivity), ERe (effective resistance), STC (spanning tree count), HE (heterogeneity), PCR, and iPCR, respectively. [Part 29/30]

id	tRank	SR	SG	NCo	ACo	ERe	STC	HE	PCR	iPCR
1121	61	627	554	638	1030	61	880	133	99	249
1122	338	642	545	666	1063	27	866	162	113	111
1123	51	656	580	680	1039	80	976.5	224	57	202
1124	210	659	571	679	1076	39	1095	178	5	126
1125	203	640	508	651	1103	11	1141.5	126	41	28
1126	310	648	498	688	1052	76	991	186.5	34	12
1127	230	689	564	752	922	106	811	229	100	189
1128	2	691	587	758	1015	110	900	271	63	158
1129	342	661	501	705	950	81	854.5	168	213	30
1130	208	688	546	757	951	91	843.5	234	74	271
1131	206	685	510	741	1001	89	1038.5	240	186	23
1132	113	666	570	692	974	29	1186	186.5	29	207
1133	163	687	520	762	1082	95	976.5	244	24	2
1134	218	690	540	753	1036	73	949	211	81	53
1135	147	643	511	655	985	36	883.5	94	90	214
1136	273	605	572	607	1074	9	953.5	42	114	80
1137	161	667	577	700	1013	94	879	168	188	85
1138	114	630	569	641	987	55	968	138	199	238
1139	170	641	534	656	1097	18	898.5	112.5	33	292
1140	46	618	507	628	1024	31	1071.5	101	106	11
1141	207	674	543	701	1029	41	1024.5	164.5	10	18
1142	129	692	578	768	993	92	1016	253	79	17
1143	138	601	509	602	1055	3	817.5	15	153	4
1144	221	611	518	619	1051	2	963.5	62	111	251
1145	84	670	588	703	971	49	957	150	201	157
1146	323	679	532	734	1083	65	843.5	190	172	191
1147	132	660	542	702	1059	75	911.5	171	157	113
1148	271	647	559	667	1008	62	1038.5	139	84	86
1149	115	621	558	633	1064	22	1055.5	73.5	229	16
1150	143	616	514	623	1071	21	968	86	69	260
1151	146	604	500	605	1022	12	980	61	155	35
1152	139	678	515	735	990	51	1024.5	199	67	48
1153	80	663	553	694	1020	59	968	189	98	165
1154	52	628	557	632	1077	7	940	77	126	155
1155	165	608	550	615	949	24	873.5	70	158	5
1156	8	633	555	645	1047	67	840	143.5	73	22
1157	263	613	595	620	1046	50	932	109.5	135	268
1158	68	677	551	725	1050	90	940	202.5	48	153
1159	72	619	517	639	1041	33	804	135	195	91
1160	264	629	552	658	1054	35	892	104	118	280

Table S31: The true ranks (tRank) and the ranks predicted by SR (spectral radius), SG (spectral gap), NCo (natural connectivity), ACo (algebraic connectivity), ERe (effective resistance), STC (spanning tree count), HE (heterogeneity), PCR, and iPCR, respectively. [Part 30/30]

id	tRank	SR	SG	NCo	ACo	ERe	STC	HE	PCR	iPCR
1161	30	683	593	737	1079	78	936.5	192	55	52
1162	296	672	527	718	1048	47	842	168	30	179
1163	316	653	585	670	1010	70	1062	160	77	133
1164	16	623	584	634	1000	45	929.5	82	156	211
1165	29	686	563	745	1075	87	1199	259	43	8
1166	10	612	525	621	1007	14	1136	63	228	61
1167	202	615	506	625	1093	5	1062	58.5	12	84
1168	193	673	560	714	1095	71	1062	182	62	7
1169	225	665	568	697	1070	72	963.5	196	13	54
1170	40	649	535	687	1062	34	849	115	179	225
1171	134	602	530	606	1078	4	834.5	41	224	34
1172	178	636	531	646	1073	77	1024.5	193	54	264
1173	110	658	566	681	1049	37	1081	143.5	85	131
1174	39	635	502	659	1090	26	846	153	37	89
1175	73	652	565	685	946	43	1024.5	164.5	56	13
1176	21	654	537	677	1057	63	904	194	278	44
1177	3	694	582	774	918	88	1129	252	46	160
1178	20	669	526	717	954	69	858.5	177	47	81
1179	164	693	499	778	1021	111	822.5	261	123	273
1180	120	617	561	627	981	17	951.5	68	193	164
1181	274	606	519	608	1094	1	1055.5	49	146	195
1182	268	626	496	642	1091	48	919	121	83	56
1183	148	603	533	603	1011	6	908.5	35	136	156
1184	42	651	528	671	1058	64	904	146	65	43
1185	160	671	589	699	1012	53	953.5	140	27	68
1186	53	650	529	673	928	57	1121.5	156	122	55
1187	175	682	513	732	1016	66	1125.5	236	14	59
1188	267	646	574	665	1060	13	1071.5	107	97	74
1189	183	638	575	652	1032	44	854.5	132	35	302
1190	151	634	562	654	1081	25	973	157	76	267
1191	272	676	522	736	1072	79	802	215	142	72
1192	64	631	590	647	1038	52	907	136.5	149	70
1193	78	657	523	684	938	60	838	172	8	306
1194	150	700	567	788	958	105	1011.5	268	61	19
1195	82	695	541	777	1053	93	1105	255	3	248
1196	169	681	573	730	1069	58	946	202.5	211	94
1197	92	639	549	648	1017	16	950	104	50	40
1198	313	620	539	629	1098	30	1062	97	26	66
1199	181	610	579	611	984	15	1121.5	37	19	183
1200	121	668	591	696	1045	40	1016	191	88	87